Bachelor of Science Thesis

The effect of Rational Heat Transfer on the behavior of Surge Vessels

Merel Toussaint

December 18, 2014

Faculty of Electrical Engineering, Mathematics and Computer Science and Faculty of Applied Sciences

.

Delft University of Technology

The effect of Rational Heat Transfer on the behavior of Surge Vessels

Bachelor of Science Thesis

For obtaining the degree of Bachelor of Science in Applied Physics and Applied Mathematics at Delft University of Technology

Merel Toussaint

December 18, 2014

Faculty of Electrical Engineering, Mathematics and Computer Science and Faculty of Applied Sciences

.

Delft University of Technology

Delft University Of Technology
Department Of
Applied Mathematics and Department of Transport Phenomena

The undersigned hereby certify that they have read and recommend to the Faculty of Electrical Engineering, Mathematics and Computer Science and Faculty of Applied Sciences for acceptance a thesis entitled **"The effect of Rational Heat Transfer on the behavior of Surge Vessels"** by **Merel Toussaint** in partial fulfillment of the requirements for the degree of **Bachelor of Science**.

Dated: December 18, 2014

Supervisor Applied Physics: _____
prof. dr. R.F. Mudde

Supervisor Applied Mathematics: _____
dr. M. Möller

Supervisor Deltares: _____
dr. ir. I.W.M. Pothof

Reader: _____
dr. J. L. A. Dubbeldam

Reader: _____
dr. B. van den Dries

Abstract

The polytropic model to describe air expansion, has been used for years to describe the behavior of surge vessels. In this thesis the alternative to describe this behavior, the Rational Heat Transfer (RHT) equation developed by Graze (1968), is extended with an estimation of all heat terms in surge vessels. The RHT model is compared to the polytropic model for isolated and non-isolated vessels and is shown to give a good estimation for the air expansion, which has been checked with measurement data from Shuweihat, a location in Abu Dhabi in the United Arab Emirates where a large pumping station is located. Calculations for the size of the surge vessel point out that the minimal volume of a surge vessel calculated with the RHT model is 10 % smaller than if the volume is calculated with the polytropic model. Furthermore, the heating of the air pocket in a surge vessel has been modeled by a numerical solution of the one-dimensional heat equation with a convective and a non linear source term. From this models can be concluded that the air in a surge vessel warms up slower than the expansion time of that vessel.

Contents

List of Figures

List of Tables

Nomenclature

Latin Symbols

ΔH	Joukowsky head change	[m]
Δv	Change in flow velocity	[m/s]
A	Surface perpendicular to heat flow	[m^2]
a	Thermal diffusion coefficient	[m^2/s]
c	Transient wave speed	[m/s]
C_p	Specific heat at constant pressure	[J/(kg K)]
C_v	Specific heat at constant volume	[J/(kg K)]
D	Diameter of the surge vessel	[m]
g	Gravitational acceleration	[m/s^2]
h_c	Convection heat transfer coefficient	[J/(s m^2 kg K)]
h_{ev}	Evaporation enthalpy	[J/kg]
h_r	Radiation heat transfer coefficient	[J/(s m^2 kg K)]
M	Molar mass	[kg/mol]
m	Mass	[kg]
N	Amount of moles	[mol]
n	Laplace coefficient	[-]
p	Absolute pressure	[bar]
p_w	Partial vapor pressure	[bar]
Q	Heat	[J]
R	Radius of the surge vessel	[m]
R	Universal gas constant	[Pa m^3 / (mol K)]

T	Temperature	[K]
t	Time	[s]
U	Overall heat transfer coefficient per unit surface	[J/(s m^2 kg K)]
v	Flow velocity	[m/s]
Z	Height of the surge vessel	[m]

Greek Symbols

ϵ	Emission coefficient for radiation	[-]
γ	Ratio of specific heats; $\frac{C_p}{C_v}$	[-]
λ	Heat conductivity coefficient	[J/(s m K)]
μ	Dynamic viscosity	[kg/s]
ν	Kinematic viscosity	[m^2/s]
ϕ''	Heat flux	[J/s m^2]
ϕ	Heat flow	[J/s]
σ	Stefan-Bolzmann radiation constant	[J/(s m^2 K^4)]

Dimensionless Numbers

Fo	Fourier; process time / effective time for heat conduction	$\frac{at}{D^2}$
Gr	Grashof; buoyancy forces / viscous forces	$\frac{D^3 g \Delta T}{\nu^2 T}$
Nu	Nusselt; total heat transfer / conductive heat transfer	$\frac{hD}{\lambda}$
Pr	Prandtl; hydrodynamic boundary layer thickness / thermal boundary layer thickness	$\frac{\nu}{a}$
Re	Reynolds; inertia forces / viscous forces	$\frac{\rho v D}{\mu}$

Subscripts

air	The property applies to air
ex	Outside the surge vessel
in	Inside the surge vessel
init	Denotes a value to be initial
steel	The property applies to steel
wall	In the wall of the surge vessel
water	The property applies to water

Chapter 1

Introduction

Large pipeline systems containing drinking water or waste water need large pumps to keep the water pressure inside the pipes steady. When the pump fails, for instance due to an electrical power outage, the pressure inside the pipe system can drop below a minimum acceptable level set by pipe manufacturers or users. To prevent this, a set of surge vessels can be installed next to the pump installation, mostly as close as possible to the pumps. A surge vessel is a large closed tank filled with water and air that is installed to supply water when pressure drops. These days, the size of the surge vessel is calculated by taking into account the polytropic process related to the expansion of the air due to supply of water to the system. The behavior of the air lies somewhere between an adiabatic process and an isothermal process, but until now there has been no further research on modeling the precise behavior of the air in the vessels. Due to this uncertainty, the savings in surge vessel volumes could be up to twenty per cent if the thermodynamic behavior could be modeled precisely (Van der Zwan et al., 2012). The profit of reducing this error can be in the range of millions of euros.

In 2012, Leruth et al. concluded that despite the fact that the hydraulic simulation program WANDA, made by Deltares ("WANDA 4.2 User Manual", 2013), can model the behavior of a complete pipeline system, the model of the air vessel was not that accurate. The measurements taken in this article to validate the model did deviate from the predicted values. In the model, the expansion of the air in the vessel was considered polytropic. In a polytropic model, no heat flow is taken into account, although heat transfer is an important part of a complete model of expanding air volumes. From several articles published by Graze (1967, 1968, 1971), it can be concluded that there is a way to take into account heat flow in air chambers in the calculations for the expanding air volume. Instead of considering a polytropic process, Graze proposed the Rational Heat Transfer (RHT) equation, that can be derived from the ideal gas law. A simplified version of this formula has been used in the Water Hammer and Mass Oscillation software program as an alternative to calculate the air volume of surge vessels (Fitzgerald & Van Blaricum, 1998).

In this thesis, the polytropic approach is questioned and the full version of the RHT model will be analyzed, including heat flow processes. The results of this model will be compared

to measurement data from recently placed surge vessels in the United Arab Emirates. Furthermore, the temperature change in the surge vessels due to diffusion, convection and condensation will be stated as a differential equation and solved numerically.

Chapter 2

Theory

2.1 Pipeline systems

In a pipeline system, several pumps are needed to make sure the pressure on the transported water is high enough to make up for the height differences or friction losses the piping system may encounter. If the pumps are working properly, the pressure in the system will stay between critical values. When the flow pressure is too low or too high, several problems may occur. With a sub-atmospheric pressure, for instance, the pipes can be damaged and the fluid inside the system can be contaminated by leakage, as stated by Thorley (2004).

There are several ways in which the system can have a sudden pressure drop, such as pump failure, or a valve closing too fast. When this happens, a pressure wave is created with low pressure. According to Thorley (2004), the speed of this pressure wave is of the same order as the speed of sound inside the fluid, where the propagation speed also depends on the material of the pipe. For a steel pipe, the propagation speed of a pressure wave in water is between 1000 and 1400 m/s. The pressure wave causes a pressure head change due to the change in flow velocity. The first drop in pressure that is noticed is the initial drop in pressure that occurs simultaneously with reduction of the flow velocity. This phenomenon is called the Joukowsky head change ΔH in m,

$$\Delta H = \frac{c}{g}\Delta v \tag{2.1}$$

with c the wave speed in m/s, g the gravitational acceleration in m/s^2 and Δv the change in flow velocity in m/s. This relation states that a 1 m/s flow velocity change will result in an approximate head change of 100 m with a wave propagation speed of 100 m/s, which is equal to a pressure of 10 bar for water. In his book, Ellis (2008) states several maximum pressures for different kinds of pipes, which are all lying in the range between 10 bar and 25 bar. That means that the pressure waves may cause serious damage to the pipeline system and measures have to be taken to reduce this problem.

Several solutions have been provided to suppress these fluid transients. Of course, measures can be taken to make the system itself stronger and more resistant to the effects of pressure waves, such as stronger pipes and avoiding valves to close too fast. Solutions can also be found in diverting the problem if it is already existent, for instance during a power cut. When this happens, a way to reduce the effect of transients in the system is placing an air vessel (Thorley, 2004). The purpose of the air vessel is to make sure the system comes to an equilibrium after pump failure without reaching the critical pressure levels. Many different types of air vessels are available, such as surge towers, vertical and horizontal vented and non-vented air vessels. Which one is chosen depends on the pipeline system that is observed, in this case the point of interest will be the vertical non-vented surge vessel.

2.2 Surge vessels

A surge vessel is a large closed tank partly filled with water and partly with air. Existing surge vessels have typical sizes of around 200 m^3 for large vessels and 10 m^3 for small ones that are used in water networks in cities. If a total volume of, say, 800 m^3 must be reached, several smaller vessels will be placed and linked for convenience in manufacturing and transport of those vessels. The vessel is placed at the start of the piping system, near the pumps, because the pumps cause the most dangerous transient waves when the power outage occurs. If this happens, a low pressure wave goes trough the system, until the location of the surge vessel. The water from the vessel is drawn into the pipes so that the water level drops. Therefore, the air inside the vessel expands and the air pressure drops.

The size of the vessel and the volume of the air in it depend on several factors that determine the pressure in the system and the extra water flow that is needed from the vessel when the pump pressure fails. The total volume of the vessel, moreover, depends on the rate of expansion of the air.

2.2.1 Laplace coefficient

As air can be regarded as an ideal gas for not too high pressures, the air pocket in the surge vessels can be modeled using the ideal gas law:

$$pV = N_{air}RT \tag{2.2}$$

where p gives the pressure, V the regarded volume, N_{air} the amount of moles of air and T the temperature of the gas, and R the universal gas constant.

To calculate the size of the vessel, the expansion of the air can be considered to be a polytropic process. A polytropic process of a closed system is described by the following pressure-volume relation (Moran & Shapiro, 2010, p. 112):

$$pV^n = C \tag{2.3}$$

with n the Laplace coefficient for air varying between 1.0 for isothermal (constant temperature) processes and 1.4 for adiabatic (no heat exchange) processes and C a constant.

This formula is used to model the air expansion, although the surge vessel can not entirely be seen as a closed system. Both values of n are used to calculate the minimum dimensions of the surge vessels. A calculation with $n = 1.0$ calculates the maximum air expansion, and a calculation with $n = 1.4$ calculates the minimum air expansion for the same drop in pressure and the minimum pressure in the pipeline. It seems convenient to use the value $n = 1.2$, that lies between 1.0 and 1.4. The value of $n = 1.2$, however, is not a correct value to base the models on, as was concluded by Leruth et al. (2012). One of the conclusions of that article was that the model that had been used had two different outcomes after comparing it to experimental results. On the one hand the results could be interpreted as such that the Laplace coefficient should be smaller than 1.2, and on the other hand the value should be larger. The reason that the Laplace coefficient for modeling the surge vessel seems to have no correct value between 1.0 and 1.4 could be that the system is not closed; water that evaporates can add mass to the regarded air volume. Heat can be lost to the surrounding tank wall and water level. If the Laplace coefficient is used to calculate the volume and pressure of an expanding air volume, the following formula is used, derived from Equation (2.3):

$$p_{init} V_{init}^{n} = p V^{n} \tag{2.4}$$

where p_{init} and V_{init} are the initial values of the air pocket and p and V the values that have to be calculated. This formula assumes the Laplace coefficient to be constant in time, although this is not necessarily the case. From this equation, the time-dependent Laplace coefficient can be calculated:

$$n = \frac{\log\left(\frac{p_{init} V_{init}^{n_{init}}}{p}\right)}{\log(V)} \tag{2.5}$$

where in this case all p and V data are known, just as the assumed initial Laplace coefficient.

2.3 Rational Heat Transfer Equation

The polytropic approximation of the behavior of the air volume in the vessel has been used for years, but it is sometimes questioned because the temperature and the heat transfer of the volume are not accounted for, though it is evident that the behavior of the surge vessels is not entirely isothermal and not entirely adiabatic, but somewhere in between. Another approach on this matter is the Rational Heat Transfer (RHT) equation proposed by Graze (1968), to take into account the heat flow in cylinders filled with air. The RHT equation is derived from the ideal gas law proposed in (2.2), and the properties of the specific heats C_p and C_v:

$$C_p - C_v = R \tag{2.6}$$

$$\frac{C_p}{C_v} = \gamma \tag{2.7}$$

where γ is defined by the ratio of the specific heats, as given in (2.7). According to Graze (1968), the concept of reversibility is given by:

$$dU = -dQ - dW \tag{2.8}$$

where dU gives the change in internal energy, dQ for the heat that goes *out* of the system, and dW the work done by the system, also defined by:

$$dW = p \cdot dV \tag{2.9}$$

Combining Equations (2.2), (2.6), (2.7), (2.9) into Equation (2.8), the following equation is found:

$$\frac{1}{\gamma - 1} d(pV) = -dQ - p \cdot dV \tag{2.10}$$

which can be rearranged and divided by dt to obtain the RHT equation:

$$\frac{dp}{dt} = -\gamma \frac{p}{V} \frac{dV}{dt} - \frac{\gamma - 1}{V} \frac{dQ}{dt} \tag{2.11}$$

In the calculation of the heat transfer to the outside of the tank, all modes of heat transfer; radiation, convection, condensation and conduction, have to be taken into account. The following equation for dQ/dt is proposed:

$$\frac{dQ}{dt} = U \cdot A \cdot (T_{in} - T_{ex}) \tag{2.12}$$

where U is the overall heat transfer coefficient per unit surface and A is the surface of the cylinder. T_{in} and T_{ex} are the internal and external temperature, respectively. The overall heat transfer coefficient can be calculated by combining the individual heat transfer coefficients of the different heat transfer processes.

To find out what kind of processes have any influence on the heat transfer into or out of the air pocket, and how large that influence is, all processes have to be mapped and calculated, so their effects can be modeled.

2.4 Thermodynamic effects

To find out which processes contribute to the heat flow in (2.11) and to determine their value, it is important to set up an energy balance for the air volume inside the surge vessel. Below, the energy balance is given between the energy that is present in the air and the heat that is moved in or out of the volume of air.

$$\frac{d(\rho_{air} V C_p T)}{dt} = \phi_{conduction} + \phi_{convection} + \phi_{condensation} - \phi_{evaporation} + \phi_{radiation} - \frac{dW}{dt} \tag{2.13}$$

with ρ the density of air, ϕ the heat flow that is transported into the air volume and W denotes the work that is done by the air pocket during the expansion of the air. This equation shows that there are several factors that influence the air temperature inside the tank. In Figure 2.1 the flow of heat is visualized. The following sections will describe derivation of the formulas needed to calculate the contribution of the different heat transfer processes to the total heat change in the volume of air. In this theory, only the heat flow from the tank wall to the air pocket is taken into account. Because there will be some wind surrounding the surge vessels, the outer temperature of the wall will be considered constant. The quantitative contribution of all heat flow processes will be calculated in Chapter 3.

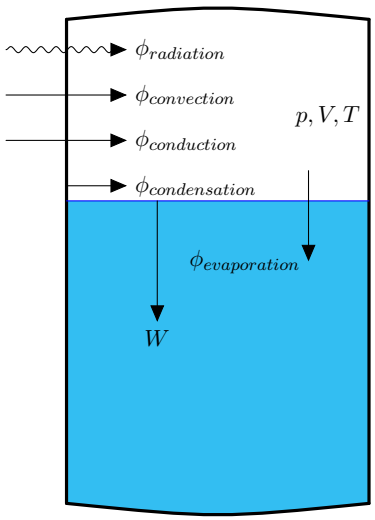

Figure 2.1: Surge vessel model with inflow and outflow of heat ϕ and work W. The outlet of the tank has been left out.

2.4.1 Conduction

Heat flow by conduction takes place on the inside and on the outside of the tank, where the outside conduction depends on the location of the surge vessel. If only the conduction inside the air volume is taken into account, an in-stationary heat balance can be constructed. This gives:

$$\frac{\partial \rho_{air} V C_p T}{\partial t} = \phi_{in} - \phi_{out} \tag{2.14}$$

where the ϕ is the heat flow in or out of the air pocket and, according to Fourier's Law, ϕ is equal to:

$$\phi_{in} = -A\lambda \left[\frac{\partial T}{\partial x}\right]_x \tag{2.15}$$

with A being the surface the heat flows through, and λ the heat conductivity coefficient. For the cylinder, the heat will flow into the tank radially from the sides and in the z-direction from the water surface and the ceiling of the tank. The distance the conductive heat travels into the air pocket is defined by the penetration depth x that depends on the time:

$$x = \sqrt{\pi a t} \tag{2.16}$$

with a the thermal diffusivity. This depth indicates the distance dx from Equation (2.15). Therefore the heat flow per unit surface from the tank wall and the water into the air pocket is decribed by:

$$\phi''_{in} = -\lambda \frac{T_{ex} - T_{int}}{\sqrt{\pi a t}} \tag{2.17}$$

2.4.2 Convection

Both on the inside and on the outside of the vessel, heat will be transported by convection. On the inside of the tank, the contributions will come from natural convection, because

there is no forced air flow inside the air volume. Natural convection is a phenomenon that is caused by the heating expansion of fluids. When the temperature of a fluid rises, the fluid expands and becomes less dense. Due to gravitational forces, the expanded fluid rises, so that a cooler part of the fluid can be heated. The convective heat flux can be calculated following Newton's cooling law (Van den Akker & Mudde, 2008, p. 145):

$$\phi'' = h_c \Delta T \tag{2.18}$$

which means a convective heat transfer coefficient is needed to calculate this flux. With the Nusselt number, this coefficient can be calculated. The Nusselt number, Nu is a dimensionless number equal to $\frac{h_c D}{\lambda}$ that gives the ratio between the total heat transfer and the heat transfer by conduction alone. In this equation, h_c is the heat transfer coefficient needed, and D is the height or the diameter of the vessel, depending on the place the convection occurs. To calculate the Nusselt number itself, two empirical formulas for natural convection on a vertical plane are stated (Van den Akker & Mudde, 2008, p. 158):

$$\mathrm{Nu} = 0.52(\mathrm{Gr} \cdot \mathrm{Pr})^{\frac{1}{4}} \quad \text{when } 10^4 < \mathrm{Gr} \cdot \mathrm{Pr} < 10^8 \tag{2.19}$$

$$\mathrm{Nu} = 0.12(\mathrm{Gr} \cdot \mathrm{Pr})^{\frac{1}{3}} \quad \text{when } \mathrm{Gr} \cdot \mathrm{Pr} > 10^8 \tag{2.20}$$

where Gr is the Grashof number, the ratio between buoyancy forces and viscous forces, and Pr is the Prandtl number, the ratio between the hydrodynamic boundary layer thickness and the thermal boundary layer thickness. For the inside of the tank the simplified case of the vertical plate is taken, because of the complicated derivation of the cylindrical case. For the water level, the equation for a horizontal plate can be used. The ceiling of the tank will not invoke natural convection, because the ceiling has a higher temperature than the air. Therefore the air just below the ceiling will not cool to sink down again. The horizontal plate free convection equation reads:

$$\mathrm{Nu} = 0.17(\mathrm{Gr} \cdot \mathrm{Pr})^{\frac{1}{3}} \quad \text{when } \mathrm{Gr} \cdot \mathrm{Pr} > 10^8 \tag{2.21}$$

This equation is assumed to describe a turbulent flow of heat and air upward.

2.4.3 Evaporation and Condensation

The volume of air is not only surrounded by tank walls, the water, too, has its influence on the temperature of the air. In equilibrium, the temperature of the water and the closed air volume ensure that the air is saturated with water vapor. A measure for the degree of saturation is the vapor pressure, that is dependent of the temperature, and can be calculated with (Lowe, 1976):

$$p_w = (a_0 + a_1 T + a_2 T^2 + a_3 T^3 + a_4 T^4 + a_5 T^5 + a_6 T^6)/1000 \tag{2.22}$$

where T is the temperature of the surrounding air and a_i are constants that can be found in Table 2.1. With this formula, the partial vapor pressure can be calculated for a saturation value of 100 %.

Table 2.1: List of constants that are used in equation (2.22).

Constant	Value	
a_0	6984.505294	
a_1	-188.9039310	
a_2	2.133357675	
a_3	-1.288580973	$\cdot 10^{-2}$
a_4	4.393587233	$\cdot 10^{-5}$
a_5	-8.023923082	$\cdot 10^{-8}$
a_6	6.136820929	$\cdot 10^{-11}$

When the pumps fail and the water level drops, the temperature drops too, and the air is still saturated, but contains less water. The amount of water vapor that is present in a kilogram of air can be calculated by (Vaisala, 2013):

$$m_{water,relative} = \frac{M_{water}}{M_{air}} \frac{p_w}{p - p_w} \tag{2.23}$$

where the molar mass ratio $\frac{M_{water}}{M_{air}}$ is equal to 0.622 and p_w is the partial vapor pressure. To calculate the amount of condensed water that turns into a mist, the relative water masses at two moments in the cooling process are subtracted and multiplied with the mass of the air. The heat that is released during this process is then calculated with the evaporation enthalpy h_{ev}:

$$\phi_{condensation} = \frac{m_{air} h_{ev}}{\Delta t} \frac{M_{water}}{M_{air}} \left[\frac{p_w}{p - p_w}|_{initial} - \frac{p_w}{p - p_w}|_{final} \right] \tag{2.24}$$

where m_{air} is the mass of the air in the regarded volume and Δt is the time difference between the 'final' and 'initial' moments.

Equation (2.24) gives a formula that calculates the condensation heat, but the physical interpretation is somewhat more complex. The difference in water vapor mass gives the amount of water vapor that has condensed. The air now contains a mist of small water droplets of radius $\sim \mu$m, which will all transport their energy to the surrounding air by conduction. Assuming the droplets have indeed a radius of 1 μm, the amount of water droplets can be calculated and the time scale to warm up their surrounding volume of air is known through the penetration depth of the heat of the water droplet into the air:

$$\sqrt[3]{\frac{V_{air}}{\text{number of water droplets}}} = \sqrt{\pi a t} \tag{2.25}$$

where the left side of the equation gives the length of the cube each droplet is in, and a is the thermal diffusion coefficient in m^2/s. In Figure 2.2 the droplet and the volume of air around it is visualized. The time scale in which the droplet transfers its energy into his own volume of air, can be calculated with a rearranged form of (2.25):

$$t = \frac{\left(\sqrt[3]{\frac{V_{air}}{\text{number of water droplets}}} \right)^2}{\pi a} \tag{2.26}$$

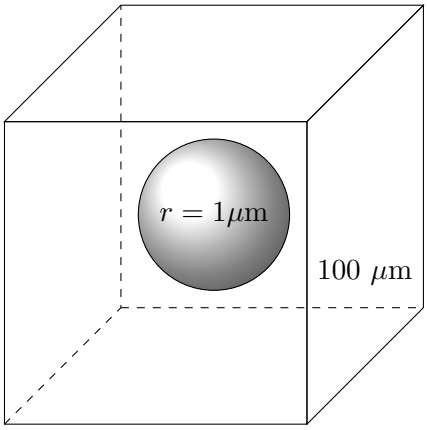

Figure 2.2: Water droplet inside its own volume of air, the evaporation energy of the droplet will warm up the volume around the droplet. The width of the droplet is approximately equal to the penetration depth.

This time can be used to determine whether the heating process of each volume of air occurs instantaneously or not.

Now, the heat distribution over this volume can be calculated to find the raise of temperature that occurs because of the condensation heat of the droplet. The energy balance that holds these terms follows below.

$$[C_p \rho V T_{init}]_{water} + [C_p \rho V T_{init}]_{air} + h_{ev} m_{water} = [C_p \rho V T]_{water} + [C_p \rho V T]_{air} \tag{2.27}$$

where T_{init} is the temperature of the air shortly after the expansion, h_{ev} is the evaporation enthalpy and T is the temperature after the distribution of the condensation energy.

Evaporation can appear when the water contains enough energy to reach the evaporation enthalpy and the air is not saturated yet. In this case, the air is saturated, and the expected drop of pressure and temperature will make the air even more saturated, which has the effect of condensation. That means that evaporation will be an issue only if the pressure or the temperature rise again. The evaporation then can be calculated in the same way as condensation, and will have a negative heat term instead.

Following equation (2.24), the enthalpy of the air is said to be the evaporation enthaplpy. In the case that the temperature drops below 273 K, the water droplets in the mist will freeze over. That gives an extra enthalpy change that transfers heat to the air.

2.4.4 Radiation

To calculate the effects of radiation, first, the radiated heat from the steel wall and the water surrounding the air volume has to be taken into account. The heat energy radiated is related to the temperature according to the radiation law of Stefan-Bolzmann:

$$\phi_r'' = \epsilon \sigma T^4 \tag{2.28}$$

with ϵ being the emission factor and σ the Stefan-Bolzmann constant. The flux out of the wall and out of the water will not entirely end up in the water vapor inside the air

volume. The heat radiated from the wall can be explained as electromagnetic waves in the infrared part of the spectrum. To obtain an estimation of the amount of heat that is absorbed by each water droplet, not only the radiation from the wall to the water droplet is important, but also the radiated heat from the water droplet outward. The net heat flow into the total mass of water in the air is then calculated by:

$$\phi_r = N_{droplets} \cdot (\epsilon_{wall} A_{droplet} \sigma T_{wall}^4 - \epsilon_{water} A_{droplet} \sigma T_{droplet}^4) \tag{2.29}$$

where $A_{droplet}$ is the spherical surface of the water droplets described in Figure 2.2 and $N_{droplets}$ is the number of droplets present in the air volume. This equation will be an overestimate for the actual heat radiated. Water vapor has its own absorption band in the infrared spectrum, and if the energy of the absorbed waves is known, the absorbed heat by the water vapor can be calculated.

2.5 Differential equations

Inside the surge vessel, temperature change takes place during the expansion of the air pocket, together with pressure change and volume change. Volume is an extensive quantity, and pressure and temperature are local quantities. The pressure differences inside the volume are caused by convection, and are relatively small, so these influences will be neglected. The temperature, however, does have some large variations inside the vessel. That means that it is interesting to know the gradient of the temperature inside the vessel as a result of the condensation factors and convection of the air. For simplicity, at first the temperature is regarded as a function of the height of the air pocket only.

To make a model of the temperature inside the vessel, first, an energy balance is made for a slice of the vessel with height dx. An energy balance with a heat production and heat flow terms is set up for each volume, which is shown in Figure 2.3.

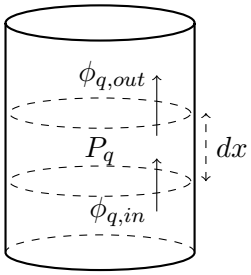

Figure 2.3: Schematic diagram of the air pocket in the surge vessel, with an energy balance of volume with height dx. The heat flow in or out is indicated by ϕ_q and the production of heat due to condensation is indicated with P_q.

The heat flow terms in this figure apply to both convection and conduction. If these terms are written down, the following expression is obtained:

$$\frac{\rho V C_p (T_{t+dt} - T_t)}{\Delta t} = \phi_{conduction,in} - \phi_{conduction,out} + \phi_{convection,in} - \phi_{convection,out} + P_{condensation} \tag{2.30}$$

Since this figure and thus the energy balance has a conduction term, a convection term and a heat production term, the heat equation can be used to describe this problem. The most standard form of the heat equation with a convection term and a production term is:

$$\frac{\partial T}{\partial t} = K\frac{\partial^2 T}{\partial x^2} + f(x,t)\frac{\partial T}{\partial x} + g(x,t) \tag{2.31}$$

with ∂x the displacement, K a constant, $f(x,t)$ and $g(x,t)$ some functions. At the left hand side, the temperature change in time is stated. The right hand side gives the conduction term, which is also known as the diffusion term, the convective term, which describes the movement of the medium that is being heated and the production term, which is nothing more than an unknown function in this formula, that influences the solution. To give this formula a bit more physical meaning, properties of the air and the different processes are added, so that the dimensions of the equation become J/s on both sides:

$$\rho C_p \frac{\partial T}{\partial t} = \lambda\frac{\partial^2 T}{\partial x^2} + \frac{\lambda \mathrm{Nu}}{Z}\frac{\partial T}{\partial x} + \phi_{condensation} \tag{2.32}$$

where the $\phi_{condensation}$ is the condensation heat term that is calculated in (2.24). The production term is thus a temperature-dependent term, which is non-linear. In the RHT model, this term is positive in most of the time steps, because the temperature drops. In this case, however, the production term is not likely to be positive because the heat equation will model an air pocket that has expanded already. Therefore the temperature will rise, and evaporation will occur in this model. That gives us a negative production term that will remove heat from the air pocket.

Chapter 3

Model Set-up

3.1 Valuation of known values

Before a model can be made with the Rational Heat Transfer (RHT) equation and all the heat process information that was obtained from Chapter 2, the known values have to be listed and evaluated. With some typical values of a surge vessel, an estimate can be made which values the model should account for, and which values can be neglected.

3.1.1 Typical values of surge vessels

The initial values of the surge vessel can be calculated for piping systems with a range of different conditions with WANDA. WANDA is a program developed by Deltares that can calculate the 1-dimensional steady and transient flows of fluids inside pipeline networks ("WANDA 4.2 User Manual", 2013). From WANDA several temperature, volume and pressure values can be obtained for a typical air vessel with an expanding air volume. In this case, a waterworks system from the town Zwolle (Figure 3.1) with a surge vessel in it is taken as an example to calculate the values. The initial conditions and the output of WANDA for different Laplace constants can be found in Table 3.1. The corresponding temperatures have been calculated using the ideal gas law, $\frac{p_1 V_1}{T_1} = \frac{p_2 V_2}{T_2}$. The values presented in this table are used to calculate the different heat contributions in the following paragraphs.

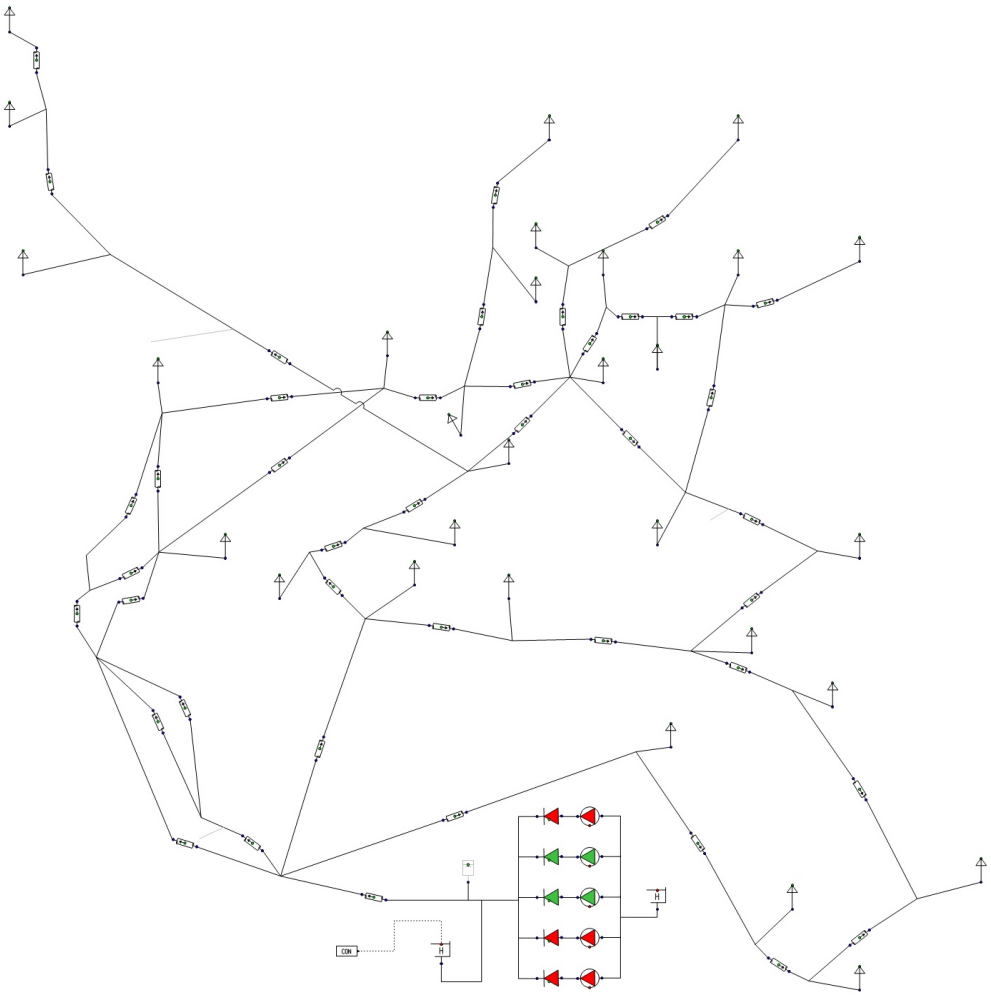

Figure 3.1: A scheme of the piping system for the waterworks system in Zwolle. On the bottom of the image, the pumps can be seen as a group of connected red and green triangles. On the left side of the pumps, the surge vessel is placed as a rectangle that is connected to the pipe. The rest of the network are all water pipes with taps. This image is fabricated by Deltares and established by WANDA.

Table 3.1: Specifications of the input and output for a typical surge vessel air expansion calculation in WANDA. The time the maximal volume and minimal pressure are reached is 101 seconds for $n = 1.0$, and 80 seconds for $n = 1.4$.

Initial conditions	Value	
Volume	18 m^3	
Floor area	3 m^2	
Initial pV = C value	1500 kJ	
Output WANDA	n =1.0	n =1.4
Air volume Initial	3.676 m^3	3.676 m^3
Air volume Maximal	12.12 m^3	9.217 m^3
Air pressure Initial	4.081 bar	4.081 bar
Air pressure Minimal	1.237 bar	1.127 bar
Temperature Initial	288 K	288 K
Temperature Minimal	288 K	199 K

3.1.2 Work done by expanding air pocket

When the air pocket expands, the pressure of the air is used to press down the water level. Work is done during this process, and this work can be used as a frame which the heat flows can be compared to. A rough estimation of the total work done by the air pocket can be done assuming that the air pocket expands with $pV^n = C$. The work can be calculated with the information from Table 3.1 and the integrated form of Equation (2.9):

$$W = \int p \, \mathrm{d}V \tag{3.1}$$

From this equation, the work W can be calculated with the MATLAB file from Appendix B.1 to be 1.79 $\cdot 10^6$ J for $n = 1.0$ and 6.86 $\cdot 10^5$ J for $n = 1.4$.

3.1.3 Total heat and conduction in tank wall

To have some perspective for the numbers that will be calculated in this chapter, the heat that can be exchanged with the air volume is calculated first. The tank wall is assumed to be manufactured of steel of 4.5 cm thickness. The total heat exchanged between the steel wall of the tank and the air is then given by:

$$[\rho C_p V]_{steel} T_w + [\rho C_p V]_{air} T_a = [\rho C_p V]_{air} T_1 + [\rho C_p V]_{steel} T_1 \tag{3.2}$$

where at the end of the process, the temperature T_1 is the final temperature for both the wall and the air. With a starting temperature T_w and air temperature T_a the final temperature becomes $T_1 = 0.998 T_w$. That means that the air almost warmed up to the starting temperature of the steel so theoretically the steel does have enough energy in it to eventually warm up the air.

Physically speaking, heat transfer from the wall of the tank can be calculated, due to the convective term in the air pocket, the air is cooling the steel wall. By calculating how fast that cooling occurs and what temperature difference arises in the tank wall, it can be determined if the change in temperature of the wall should be taken into account. In Figure 3.2 the heat flow through the interface between air and steel is schematized. The visualization from Figure 3.2 can be put in an energy balance, where the conductive flow is given by Fourier's law $\phi_{cond} = -\lambda \frac{dT}{dx}$, with dx the penetration depth ($\sqrt{\pi a_{steel} t}$):

$$\phi_{cond} = -\lambda_{steel} \frac{T_{wall} - T_i}{\sqrt{\pi a_{steel} t}} = \frac{\mathrm{Nu} \lambda_{air}}{D} T_i - T_{air} = \phi_{conv} \tag{3.3}$$

which can be written as:

$$T_i = \frac{\lambda_{steel} D T_{wall} + \mathrm{Nu} \lambda_{air} \sqrt{\pi a_{steel} t} T_{air}}{\mathrm{Nu} \lambda_{air} \sqrt{\pi a_{steel} t} + \lambda_{steel} D} \tag{3.4}$$

where Nu is roughly estimated to be 200 following the formula in Equation (2.20), λ_{steel} is equal to 16 J/(s m K), and a_{steel} is equal to 4 $\cdot 10^{-6}$ m^2/s. In the most extreme situation, the wall temperature is 288 K and the air temperature 199 K (Table 3.1). This formula can be used to calculate the drop in temperature of the interface as a function of time. This process gives a decay in temperature that can be found in Figure 3.3.

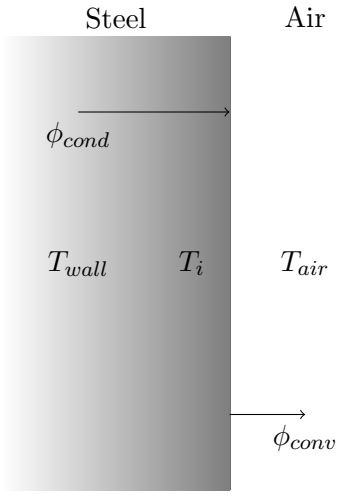

Figure 3.2: A part of the steel wall that is in contact with the air. A conductive heat flow ϕ_{cond} goes through the steel to the air-steel interface and a convective heat flow ϕ_{conv} goes from the interface into the air. T_i is the temperature of the steel on the interface.

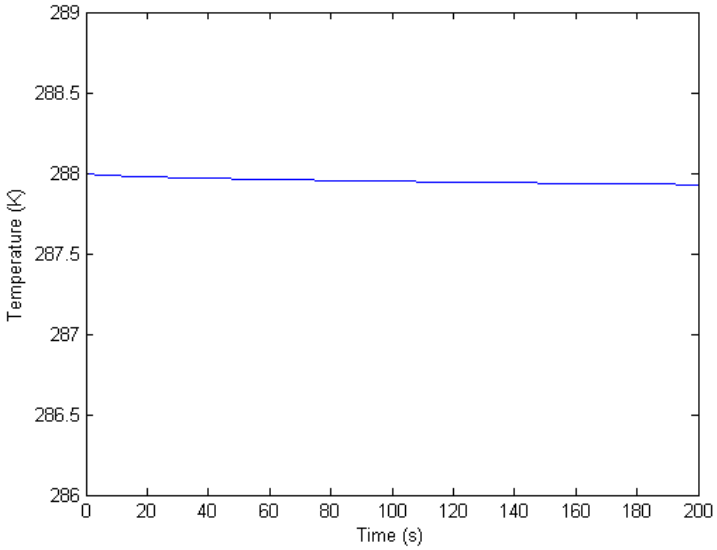

Figure 3.3: The temperature T_i on the steel-air interface on the inside of the tank wall for a wall temperature of 288 K and an air temperature of 199 K.

From Figure 3.3 it can be seen that after 200 seconds the temperature on the interface between air and steel has dropped less than 0.1 K. As stated above and by Graze (1968), the temperature on the inside of the tank wall can be considered constant. The penetration time for a wall thickness of 4.5 cm is 160 seconds, so at that point in time the outside of the tank wall will have a temperature difference. The significance of this difference, however, is very low, as can also be concluded from Figure 3.3. The MATLAB code used to do these calculations can be found in Appendix B.2.

3.2 Calculation of heat transfer processes

In this section, all processes explained in Chapter 2 will be evaluated and their contribution to the total heat transfer will be given. As in Chapter 2 many of the heat contributions are given as fluxes ϕ'', the surface of the tank for instance is needed to calculate the total heat contribution. After the standard information about the surge vessel is known, the different heat transfer processes discussed in Chapter 2 will be calculated quantitatively. In these calculations only the minimum and maximum values will be taken into account, so there may be some estimation errors regarding this approach.

3.2.1 Conduction

To calculate the order of the influence of the conduction on the total heat change of the air, it is easier to regard the heat flow by conduction through a 'plate of air'. The theory used to get a heat loss term is the penetration theory, to describe in-stationary heat flow. This theory can be used if the Fourier number (Fo) is lower than 0.1. Together with a radius of about 1 m and a thermal diffusion coefficient of $2.11 \cdot 10^{-5}$ m^2/s the Fourier number after a typical time of 100 seconds is $5.298 \cdot 10^{-4}$. That means that the penetration theory can be applied to this problem. According to (Van den Akker & Mudde, 2008, p. 122), the heat outflow in a plate can be calculated:

$$\phi''|_{x=0} = -\lambda \left[\frac{\partial T}{\partial x}\right] = \lambda \frac{T_1 - T_0}{\sqrt{\pi a t}} \tag{3.5}$$

with ϕ'' the heat flux. The total temperature drop is around 88 K, so the heat outflow through some surface at some time t is $285/\sqrt{t}$ J/m^{2}s. In a total time of 100 seconds, the heat transferred by conduction is estimated to be in the order of 10^4 J.

3.2.2 Convection

With the formulas stated in Chapter 2 the convective flux on the inside of the tank can be calculated with the Nusselt number (Equations (2.21), (2.20) and (2.18)). For this situation, Pr $\cdot$ Gr is in the order of $2.03 \cdot 10^9$ so the turbulent equation for Nu can be used, and this gives Nu = 152. This already indicates that all heat transfer processes are a factor 152 more significant than the contribution of conduction, from the definition of the Nusselt number. This can be used to calculate h_c and with that value the heat flux, which is equal to $\phi'' = 722$ J/m^{2}s. In total, the contribution of convection to the heat transfer can be estimated to be almost 10^6 J.

3.2.3 Evaporation and condensation

The air in the tank is saturated, and because the lower temperature causes a lower partial vapor pressure, water will condense. Following the formulas given in Chapter 2, first the molair mass fraction should be calculated. This is equal to 622 kg$_{air}$/kg$_{water}$ for air and water (Vaisala, 2013). The partial vapor pressure p_w at an air temperature of 200 K is equal to $1.29 \cdot 10^{-4}$ bar (Moran & Shapiro, 2010) and the air pressure is 1.270 bar. For a

temperature of 288 K that is $p_w = 0.0171$ bar and $p = 4.081$ bar. That gives us a mass fraction of $2.6 \cdot 10^{-3}$ kilograms of water per kilogram of air for the initial temperature and pressure. For the final temperature and pressure, the fraction is equal to $7.1 \cdot 10^{-5}$ kilograms of water per kilogram of air. These values give an added mass of liquid water of 0.0459 kg for an air mass of 18.15 kg.

This mass of water is distributed over the tank as a mist with each droplet containing its condensation energy. According to the formula of the penetration time, (2.26), the penetration time of the small volume containing each water droplet is in the order of 10^{-4} seconds. That means that the heating of this small volume and thus of the whole volume can be assumed instantaneous. Following (2.27) and with a condensation enthalpy of about 2200 kJ/kg, the final temperature of the air and the water droplets is 241.6 K. The amount of energy added to the air is $1.01 \cdot 10^5$ J.

3.2.4 Radiation

To calculate the contribution of the radiation of heat into the air pocket, the heat flux out of the steel wall can be calculated. For a temperature of 288 K, the constant of Stefan-Boltzmann $\sigma = 5.67 \cdot 10^{-8}$ J/(s m^2 K^4) and an emission coefficient of 0.7, the heat flux is equal to 273 J/(m^2 s).

From (2.29), the heat flow into the water droplets can be obtained, which will transfer their heat into the air. The amount of droplets can be calculated by dividing the air volume by the estimated volume of a droplet, and this gives an amount of order 10^{12}. With this information an overestimated value of the heat gained from radiation can be calculated. This value is equal to $2.9 \cdot 10^3$ W. For 100 seconds, the total radiation energy transferred to the air is of order 10^5 J. In this calculation the view factors for instance have not been taken into account, so the actual value will be smaller than the calculated value. Therefore, the radiation term will not be taken into account by making the model.

3.2.5 Comparing different heat transfer contributions

From the previous sections it can be concluded that all processes considered have an influence on the total heat transfer. All four processes have an estimated heat transfer that is comparable. Free convection has the largest contribution and conduction the smallest. In the model calculations, free convection, condensation and conduction are included, because the radiation term can only be overestimated due to the view factors that can not easily be calculated for 10^{12} water droplets. The MATLAB code that calculates these estimations can be found in Appendix B.3.

3.3 Model of Rational Heat Transfer equation

In this section, the way the RHT equation is modeled, is explained. Several simplifications and errors are mentioned.

3.3.1 Heat part of the RHT equation

Now that an estimation has been made for the heat transfer that belongs to every process, the significant processes can be put into the heat transfer coefficient of the Rational Heat Transfer equation (2.12). In this equation, all heat contributions are assumed linearly dependent on the temperature. In the previous sections, it can be seen that this assumption is not correct for all processes. In the conduction process (3.5), a linear dependency can be found and the factor $\frac{\lambda}{\sqrt{\pi at}}$ can be considered a heat transfer coefficient. In the case of natural convection, however, the heat transfer coefficient depends on the Nusselt number, which is, through the Grashof number, dependent of the reciprocal of T. Condensation, furthermore, depends on a polynomial of T because of the dependency of the partial vapor pressure of water. Because of these differences, the different processes can not be generalized as in equation (2.12), but should be regarded individually:

$$\begin{aligned}\frac{dQ}{dt} = &-\lambda\frac{\Delta T}{\sqrt{\pi at}}\left(\frac{2}{4}\pi D^2 + \pi DZ\right) - \frac{\mathrm{Nu}}{D}\lambda\Delta T\left(\frac{1}{4}\pi D^2 + \pi DZ\right) \\ &-0.622 h_{ev} V\rho\frac{p_w(T_{init})}{(p - p_w(T_{init}))} + 0.622 h_{ev} V\rho\frac{p_w(T_{final})}{(p - p_w(T_{final}))}\end{aligned} \tag{3.6}$$

where p_w is calculated from (2.22) and Nu from (2.20) and (2.20) for the walls and the water level, respectively. The term between the round brackets is the calculation of the surface of the tank and the water through which the heat flows. Because convection does not occur at the ceiling of the tank, the ground surface is only counted once in the convection term. The minus signs are put in because the $\frac{dQ}{dt}$ term considers the heat flow out of the air pocket.

In this formula, several approximations are made. For conduction, the penetration theory from Van den Akker & Mudde (2008) may not be applicable for radial use in cylinders. As a result to that, the $\sqrt{\pi at}$ value used in (3.5) may give an error in the calculations. Furthermore, the heat conduction is dependent on the temperature difference between the tank wall and the air inside the tank. Because the conductivity of the air is low compared to other materials, the conduction of heat will not penetrate the whole cylinder. If conduction alone is regarded, the penetration depth $\sqrt{\pi at}$ for a time t of 100 seconds is around 8 cm. This heat will then be spread through the whole tank by natural convection.

The convection term has a heat transfer coefficient that makes use of the Nusselt number, the Nusselt number in this case is calculated by using Equation (2.20) for a vertical plate for the walls of the tank. The surfaces of the tank can not be seen as flat, so this, too, may give an error in the calculations. The size of this error is hard to investigate, because no formula for cylindrical structures could be found in the literature.

Condensation heat transfer is measured in the total volume of the air pocket. In this volume, the heat that is released at a certain temperature can be calculated with the partial vapor pressure. The formula to calculate the partial vapor pressure, (2.22), is an empirical polynomial formula and gives an error of less than 1% (Lowe, 1976). Secondly, in this calculation, the extra energy obtained when the droplet freezes over is not accounted for. That means that the value of the condensation heat could be slightly higher than estimated. The fusion energy of water is 334 kJ / kg, which is only slightly more than 10 % of the evaporation enthalpy. As the temperature will not always be lower than 273 K, the error of this estimation will be less than 10 %.

3.3.2 Implementation of the total RHT equation

Now that the heat part of the RHT equation is fit to be used in a model, the rest of the equation (2.11) can be considered. For convenience, at first, the air volume is regarded as a whole, with no temperature variations inside. This means that the differential equation will only be solved in time. As the volume of air is regarded as a single cell, the equation can be solved in an iterative process. To model the behavior of the surge vessel, every iteration the pressure on that time is gained from WANDA. This information is used to calculate the volume from the next time step, with an alternative writing of the RHT equation (2.11):

$$\frac{dV}{dt} = -\frac{1}{\gamma}\frac{V}{p}\frac{dp}{dt} - \frac{\gamma - 1}{p\gamma}\frac{dQ}{dt} \tag{3.7}$$

where instead of $\frac{dp}{dt}$, $\frac{dV}{dt}$ is calculated. The heat term is calculated with the initial value of the temperature. In the first time step, this term is equal to zero, because there has not been any temperature change. Then the volume and pressure values can be used to calculate the new value of the temperature with the ideal gas law (2.2). These calculations are implemented in MATLAB, and can be found in Appendix B.4. The connection that has been made with WANDA to obtain values from the WANDA models can be found in Appendix B.5.

3.3.3 Minimal volume for surge vessels

To calculate the dimensions of the surge vessel that are needed meet the safety restrictions, there are two factors that should be dealt with. The pressure on the system can not be lower than 1 bar because then cavitation will occur and pipes could be damaged because of the sub-atmospheric pressure, and the water level must be higher than the diameter of the main supply line to prevent the surge vessel from draining down. With an initial $pV = C$ value, an optimization process can be used to calculate the minimum value of the surge vessel that is needed. This optimization process is similar to the process used by Van der Zwan et al. (2012) and is called the bisection method. In this method, for the minimum water level and the minimal pressure, maximum and minimum initial C values are defined. With these extreme values and the bisection method, the optimum initial C value can be found for both the minimum pressure and the minimum water level for several surge vessel volumes. This gives a region with surge vessel volumes and their initial C values that are acceptable.

This has always been done for the two values of the Laplace coefficient, and it also has to be done for the RHT approach. From this optimization process it can be concluded whether the RHT solution does predict a lower surge vessel volume. The optimization process starts with a calculation of minimum pressures and water levels from given initial C values and surge vessel volumes. If these data sets are combined, the minimum acceptable surge vessel volume is known. For the case explained in Section 3.1.1, surge vessel volumes from 6 m^3 until 18 m^3 are used.

3.4 Validation of the RHT model

Next to setting up the model, validation of the model is as important. To verify the model, a set of measurement data has been used. The experiment was done in Shuweihat, in the United Arab Emirates in July 2014.

3.4.1 Shuweihat surge vessel installation

To validate the RHT model with results of an actual surge vessel, the model is applied to a piping system which has been placed in the United Arab Emirates in 2006 and which was analyzed by Leruth et al. (2012). As a result of an increase of capacity the system, additional surge vessels have been installed, and new measurements have been performed during commissioning tests in 2014. The Shuweihat part of the system consists of eight surge vessels of 121.4 m^3 each, and one stand-by vessel. The data of this piping system is obtained by the commissioning tests of the system in 2014 during a full pump trip. In this experiment, the air pressure the water level and the temperature inside the vessel are measured. The starting pressure is around 16 bar and the initial water level is around 9 m. The experiment is done between 7 a.m. and 12 p.m. and in this time three pump trips were initiated, which all lasted between 1000 and 4000 seconds. The pump trip that is used for the validation started at 9:27 a.m..

To compare this data with the RHT model, the WANDA input is adjusted to this specific installation, because as a difference to the network model this installation has eight surge vessels. The values that are used as input for the model can be found in Table 3.2. These values are obtained from the initial values of the measurements.

Table 3.2: Specifications of the input for the surge vessels that are placed in Shuweihat, United Arab Emirates. In total, eight vessels are installed, each vessel has the following properties.

Initial conditions	Value
Volume	121.4 m^3
Floor area	10 m^2
Initial pV = C value	38000 kJ
Outside and water temperature	313 K
Initial air temperature	313 K

3.5 Mathematical approach

The temperature distribution in the air vessel can be calculated using equation (2.32). In this model, a one-dimensional approach will be used, because in the amount of time left to do these calculations, the modeling of the different terms was considered more important than the modeling in two or three dimensions. To make a model of this equation, it has to be discretized in space (x) and time (t).

3.5.1 Discretization in space (x)

Space is, in this case, the height of the surge vessel. This domain will be divided in N equal parts with length $h = \frac{Z}{N}$. The temperature will be discretized in space (x) such that T_i is the temperature in the ith grid point on height ih. This discretization is shown in Figure 3.4. The boundary conditions we have on this domain are the water temperature T_{water} at $x = 0$ and the wall temperature T_{wall} at the ceiling of the tank at $x = Z$. The second order derivative from (2.32) can be approximated with a central difference method (Vuik et al., 2006). For this term we can write the following equation:

$$\lambda \frac{\partial^2 T}{\partial x^2} = \lambda \frac{T_{i-1} - 2T_i + T_{i+1}}{h^2} + O(h^2) \tag{3.8}$$

where the values for T_0 and T_N follow from the boundary conditions. The truncation error of this method is $O(h^2)$ (Haberman, 2014).

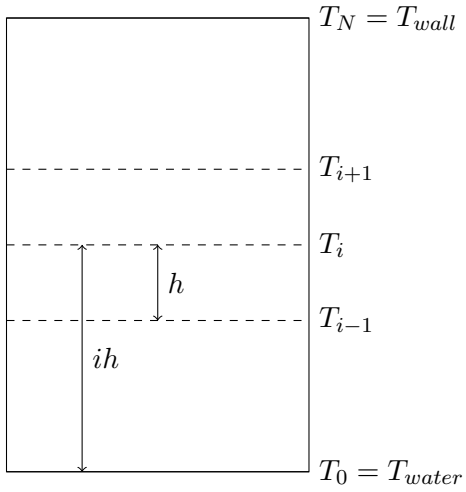

Figure 3.4: Schematic view of the discretization of the surge vessel with the several grid points.

The first order derivative from (2.32) can be approximated with several numerical methods. The centered difference method can be a useful method with an $O(h)^2$ truncation error:

$$\frac{\lambda \mathrm{Nu}}{Z} \frac{\partial T}{\partial x} = \frac{\lambda \mathrm{Nu}}{Z} \frac{T_{i+1} - T_{i-1}}{2h} + O(h^2) \tag{3.9}$$

This method has a truncation error of $O(h^2)$, so if h approaches zero, the error will reduce quadratically. Vuik et al. (2006) explains that oscillations may occur with this method when $h \leq M$, where M depends on the factor $\frac{\lambda \mathrm{Nu}}{Z}$. An upwind difference method does not have any constraints on h, and will give an approach without oscillations. The upwind difference method can be applied to the convective term as:

$$\frac{\lambda \mathrm{Nu}}{Z} \frac{\partial T}{\partial x} = \frac{\lambda \mathrm{Nu}}{Z} \frac{T_{i+1} - T_i}{h} + O(h) \tag{3.10}$$

This method has a truncation error of $O(h)$, which means that if h approaches zero, the truncation error will reduce with the same speed.

To make these contributions solvable, matrices are formed from the several numerical integration methods. The equation that has to be solved after discretization in the x-direction is:

$$\frac{dT}{dt} = AT + r \tag{3.11}$$

where A is a matrix with all integration methods in it and r is a vector with the boundary conditions in it.

$$A = \frac{\lambda}{h^2}\begin{pmatrix} -2 & 1 & & \varnothing \\ 1 & -2 & 1 & \\ & \ddots & \ddots & \ddots \\ \varnothing & & 1 & -2 \end{pmatrix} + \frac{\lambda \mathrm{Nu}}{Zh}\begin{pmatrix} -1 & 1 & & \varnothing \\ 0 & -1 & 1 & \\ & \ddots & \ddots & \ddots \\ \varnothing & & 0 & -1 \end{pmatrix}, r = \begin{pmatrix} T_{wall}\frac{\lambda}{h^2} \\ 0 \\ 0 \\ T_{water}\left(\frac{\lambda}{h^2} + \frac{\lambda \mathrm{Nu}}{Z}\right) \end{pmatrix} \tag{3.12}$$

3.5.2 Discretization in time (t)

For the discretization in time (t), the time interval is divided in several small time steps (order 0.01 or smaller). The method that is used to integrate the differential equation (3.11) is a two-step method (Vuik et al., 2006). The convective and conductive terms can be implemented explicitly or implicitly. In this case, the conductive term is treated implicitly and the convective term is treated explicitly. This method is implemented in the following way, including the discretizations of the conduction term and the convection term:

$$\rho C_p \frac{T_i^{n+1} - T_i^n}{k} = \lambda \frac{T_{i-1}^{n+1} - 2T_i^{n+1} + T_{i+1}^{n+1}}{h^2} + \frac{\lambda \mathrm{Nu}}{Z}\frac{T_{i+1}^n - T_i^n}{h} \tag{3.13}$$

where k denotes the length of each time step, the superscript n and $n+1$ denote the time and subscript i, $i-1$ and $i+1$ denote the place of the point of which the temperature is defined. This difference equation is linear, and can therefore be solved numerically with a the -operator in MATLAB, and is then iterated over a number of time steps. The temperature on every height of the air pocket on the next time step is calculated following:

$$T^{n+1} = (I - D)^{-1}\big((I + C)T^n + r\big) \tag{3.14}$$

where T^n is a vector of all temperature values on different heights on time $t = n$, r is the vector with boundary conditions for this equation, which is the same as in Equation (3.12), I is a matrix that contains the left hand side values of Equation (3.13), D contains the values of the diffusive part (conduction) and C contains the convective terms. The matrices I, D and C are given by:

$$I = \frac{\rho C_p}{k}\begin{pmatrix} 1 & 0 & & \varnothing \\ 0 & 1 & 0 & \\ & \ddots & \ddots & \ddots \\ \varnothing & & 0 & 1 \end{pmatrix}, D = \frac{\lambda}{h^2}\begin{pmatrix} -2 & 1 & & \varnothing \\ 1 & -2 & 1 & \\ & \ddots & \ddots & \ddots \\ \varnothing & & 1 & -2 \end{pmatrix}, C = \frac{\lambda \mathrm{Nu}}{Zh}\begin{pmatrix} -1 & 1 & & \varnothing \\ 0 & -1 & 1 & \\ & \ddots & \ddots & \ddots \\ \varnothing & & 0 & -1 \end{pmatrix} \tag{3.15}$$

where k denotes the time step and h the height difference.

3.5.3 Source Term

The source term does not need a numerical integration method, but because the term is not linear, it has to be linearized. According to Patankar (1980) the source term should be of the form:

$$S = S_c + S_p T \quad \text{with } S_p \leq 0 \tag{3.16}$$

with S_c the constant part of the source term and S_p the part that is multiplied with T.

The source term consists of two parts for two different time steps. For both time steps the formula will be dependent of T_i. Without linearization, the production term is:

$$S = 0.622 h_{ev} V \rho \frac{p_w(T_i)}{p - p_w(T_i)} \tag{3.17}$$

with p_w a the polynomial from (2.22). Because of this polynomial, the linerarization of the equation will be done by excluding T_i:

$$S = 0.622 h_{ev} V \rho \frac{p_w(T_i)}{T_i(p - p_w(T_i))} \cdot T_i \tag{3.18}$$

The actual condensation contribution is then calculated by subtracting the water mass on $t = n + 1$ from $t = n$, then the source term S^{n+1} on time step $n + 1$ becomes:

$$S^{n+1} = 0.622 h_{ev} V \rho \frac{p_w(T_i^n)}{T_i^n(p - p_w(T_i^n))} \cdot T_i^n - 0.622 h_{ev} V \rho \frac{p_w(T_i^{n+1})}{T_i^{n+1}(p - p_w(T_i^{n+1}))} \cdot T_i^{n+1} \tag{3.19}$$

This term is negative when the temperature difference is positive, because then the water evaporates, which costs energy.

With this term, the complete difference equation becomes:

$$\begin{aligned} \rho C_p \frac{T_i^{n+1} - T_i^n}{k} = \lambda \frac{T_{i-1}^{n+1} - 2T_i^{n+1} + T_{i+1}^{n+1}}{h^2} + \frac{\lambda \mathrm{Nu}}{Z} \frac{T_{i+1}^n - T_i^n}{h} + \\ 0.622 h_{ev} V \rho \frac{p_w(T_i^n)}{T_i^n(p - p_w(T_i^n))} \cdot T_i^n - 0.622 h_{ev} \rho \frac{p_w(T_i^{n+1})}{T_i^{n+1}(p - p_w(T_i^{n+1}))} \cdot T_i^{n+1} \end{aligned} \tag{3.20}$$

where the conductive term is solved implicitly, the convective term is solved explicitly and the production term has both an explicit and an implicit part. In a matrix-vector format, with separated T^{n+1} and T^n parts, this equation looks like:

$$\big(I - D + P(T^{n+1})\big)T^{n+1} = \big(I + C + P(T^n)\big)T^n + r \tag{3.21}$$

with $P(T^n)$ the left part of Equation (3.19) calculated with T^n on every point. Equation (3.20) is not linear an can not be solved as such. Therefore, the fixed point iteration method is used to solve the heat equation with a non linear production term.

3.5.4 Fixed point iteration method

The fixed point iteration method is used to solve difference equations with non-linear terms that are dependent on the temperature. The nonlinear terms have to be linearized

first, which is done for the source term in Equation (3.19). The fixed point iteration is an iteration that is performed every time step, to calculate the values of the nonlinear terms along with the new values for the temperature (Kuzmin & Möller, 2004). Within every time step, the second iteration starts with the calculation of a residual:

$$R^m = \big(I + C + P(T^n)\big)T^n + r - \big(I - D + P(T^m)\big)T^m \tag{3.22}$$

where m is the integer that denotes the the inner iteration. In this iteration, for $m = 0$, T^m is equal to T^n.

With this residual, a new estimation of the temperature T^m can be made, by calculating a ΔT^m which has to be added to T^m to obtain a new value for T^m which will be a better estimate for T^{n+1}.

$$\Delta T^m = (I - D + P(T^m)^{-1}R \tag{3.23}$$

This process will be done until the residual converges to a value that is 0.1 % of the starting value for every time step. Then the inner iteration is done and T^m is equal to T^{n+1}. The MATLAB code containing the implementation of this method can be found in Appendix B.6.

3.5.5 Error Analysis

For every mathematical model, it is important to do an error analysis to learn the reliability of the found solution. There are several different errors that can be made during numerical modeling. Iteration errors occur for instance when the convergence criterium is a small difference between two iterates while the iterations converge slowly. These errors are normally at least an order of magnitude smaller than discretization errors (Ferziger & Peric, 2002). Discretization errors occur when the grids used are not fine enough. Furthermore, modeling errors occur in models that describe physical systems, and can only be estimated if experimental data is available. Ferziger & Peric (2002) propose a formula to estimate discretization errors. This error estimation is based on different errors that can be measured when solutions are compared that have been calculated with different grids. These grids should be refined for each calculation in a substantial and systematic way, which means the grid should be refined with at least 50 %. The simplest way to do this is to compare the finest grid available with a certain node distance h and compare its results to the results with node-distance $2h$ and $4h$. The error can be calculated with:

$$\varepsilon_h \approx \frac{||T_h - T_{2h}||}{r^p - 1} \tag{3.24}$$

with h the smallest node distance and T_h the temperature solution with this distance. The value of r is the factor by which the grid density is increased, in this case, $r = 2$. For p the following formula is stated:

$$p = \frac{\log\left(\frac{||T_{2h} - T_{4h}||}{||T_h - T_{2h}||}\right)}{\log\ r} \tag{3.25}$$

This number denotes the order of the error made by the discretization. $||T_h||$ gives the norm of the vector T_h.

With the formulas for the estimation of grid-size errors, an error calculation can be set up. Formulas (3.24) and (3.25) will be filled in with the temperature vectors for different grids on the last time step. The calculations will be done for a grid size between 200 and 2000 cells and between 1000 and 1000000 time steps.

The error that is calculated is the root of the sum of all errors squared, which means that the error value can be large because one grid cell has a relatively high error. The MATLAB code with which the error analysis has been done can be found in Appendix B.6.1.

Chapter 4

Results

4.1 RHT model

4.1.1 Temperature, pressure and volume values

From the Rational Heat Transfer model, several results were obtained. The graphs found in Figure 4.1 compare the development of pressure, volume and temperature from the RHT model with the RHT model for insulated vessel walls and the outcomes from WANDA. For all quantities it can be seen that both RHT values lie between the values of the WANDA model. That means that indeed the values gained from the RHT model are part of a polytropic process that lies between an isothermal and an adiabatic process, as was expected. The values that WANDA calculated from the Laplace coefficients of $n = 1.0$ and $n = 1.4$ are considered to model the extreme behavior of the surge vessel.

In all graphs the four lines are different, although in the first 40 seconds a similarity can be found between the adiabatic volume expansion and the RHT model values for pressure, volume and temperature. This is a plausible result, as the different heat transfer processes depend on the difference between the current temperature and the initial temperature. This difference is not that significant in the beginning of the volume expansion, so the heat transferred into the air is not that significant. This means the RHT process can be considered an adiabatic process during this time. The RHT lines for the insulated vessel walls lie very close to the adiabatic line. This can be explained because a big part of the heat transfer into the volume vanishes when the walls are insulated, so the process is almost adiabatic.

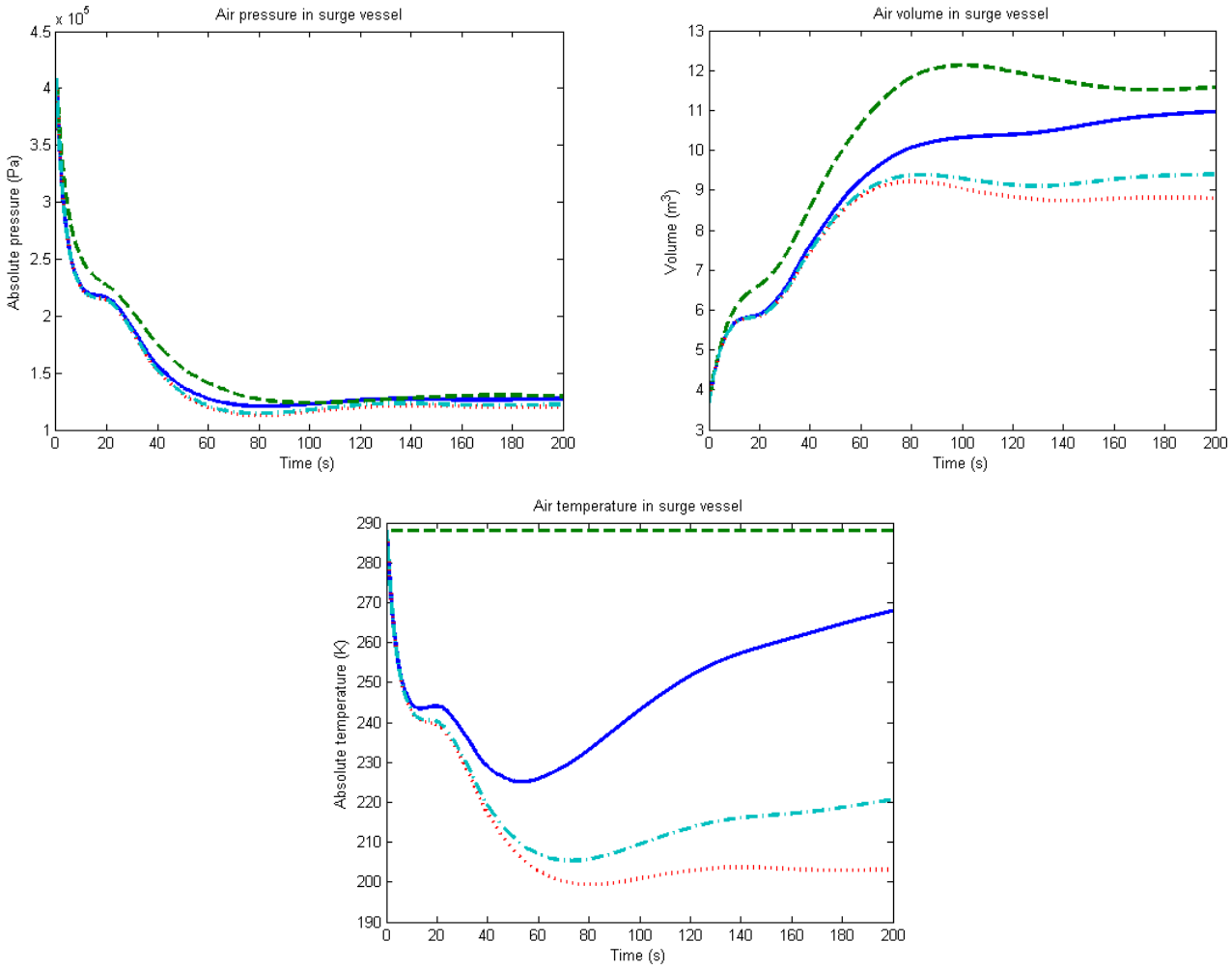

Figure 4.1: Values of air pressure, air volume and air temperature of the RHT equation (solid line) compared to the RHT model outcome for insulated walls (dash-dotted line) and the WANDA model with $n = 1.0$ (dashed line) and $n = 1.4$ (dotted line).

4.1.2 Heat flows

The final RHT model includes the heat flow components that were estimated in Chapter 3. In this Chapter, too, an estimate was made for the total work done by the expanding gas. The heat contributions and the work have been plotted in Figure 4.2. In this graph it can be seen that the convective term is highest as was expected after the estimations done in Chapter 3. The other contributions lie close together.

In Table 4.1 the total energies of the different processes can be found, the values are gained from integrating the graphs from Figure 4.2. Also the mean heat flows per second are given. In absolute terms, these values differ from the estimations in Chapter 3, but relatively, the values match the estimations; the contributions of conduction and condensation are still less than 10 % of the contribution of convection.

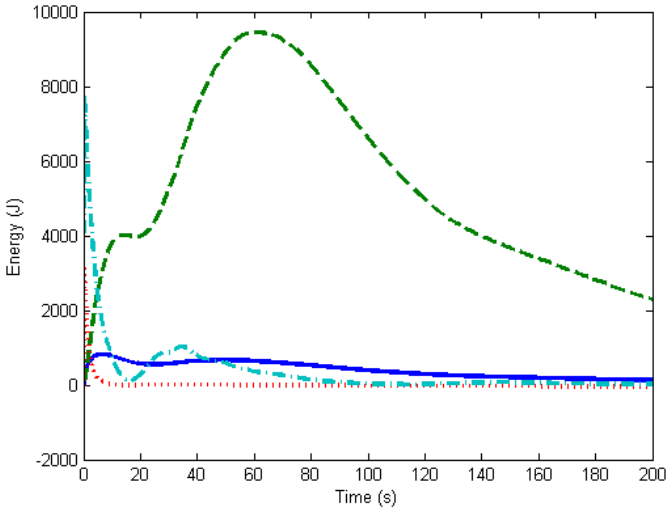

Figure 4.2: Heat contributions in time of conduction (solid line), convection (dashed line) and condensation (dotted line) and the work done by the expanding volume (dash-dotted line).

Table 4.1: Total heat flow from the different processes and work done by the air pocket and the energy that is transported into the system or the work done by the system per second.

Energy contribution	Sum	Mean value
Conduction	$1.64 \cdot 10^6$ J	410 J/s
Convection	$2.14 \cdot 10^7$ J	$5.34 \cdot 10^3$ J/s
Condensation	$2.18 \cdot 10^4$ J	5.46 J/s
Work	$1.40 \cdot 10^6$ J	350 J/s

4.1.3 Laplace coefficient

Because the Laplace coefficient is a constant in the WANDA model, and one of the expectations was that the Laplace coefficient may vary in time, in Figure 4.3 the Laplace coefficient is calculated from the pressure and volume data obtained from the RHT model, and from the pressure and volume data for the insulated surge vessel. For this calculation, a starting value is needed. Starting value $n = 1.4$ and $n = 1.0$ have been used to calculate the time variable Laplace coefficient of the RHT values. Choosing $n = 1.4$ as a starting point seems logical, because the graphs in Figure 4.1 show that the RHT curve has values similar to the values of the curve of $n = 1.4$. The graph shows that the Laplace coefficient of the insulated RHT line does indeed lie near the $n = 1.4$ line.

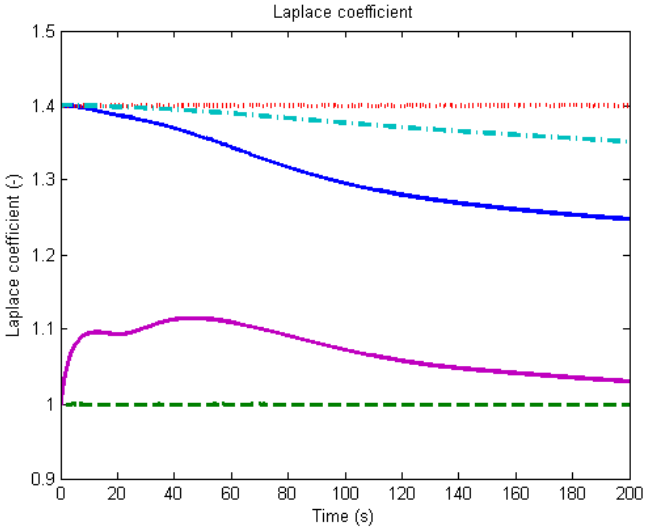

Figure 4.3: Laplace coefficient values calculated from the RHT equation with starting value $n = 1.4$ (solid line) and with insulated vessel walls (dash-dotted line) plotted next to $n = 1.0$ (dashed line) and $n = 1.4$ (dotted line). The graph from the RHT equation with starting value 1.0 also has a solid line, but starts at $n = 1.0$.

4.1.4 Minimal sizes of surge vessel

For the network in Zwolle, an optimization calculation has been performed, to see if the RHT model allows a smaller surge vessel volume than the polytropic models. In Figure 4.4 the optimization curve can be found. The triangle on the right side of the graph shows the acceptable volumes of surge vessels with their corresponding range of acceptable initial C values. The upper bound of this triangle show the acceptable initial C values given by the minimum water level in the tank. The acceptable initial C values given by the minimum pressure in the pipes are represented by the lower bound of the triangle. In this graph it can be seen that the adiabatic model defines the pipe pressure boundary and the isothermal model defines the water level boundary. Furthermore the graph shows that the triangle bounded by the RHT model line is larger than the triangle bounded by the

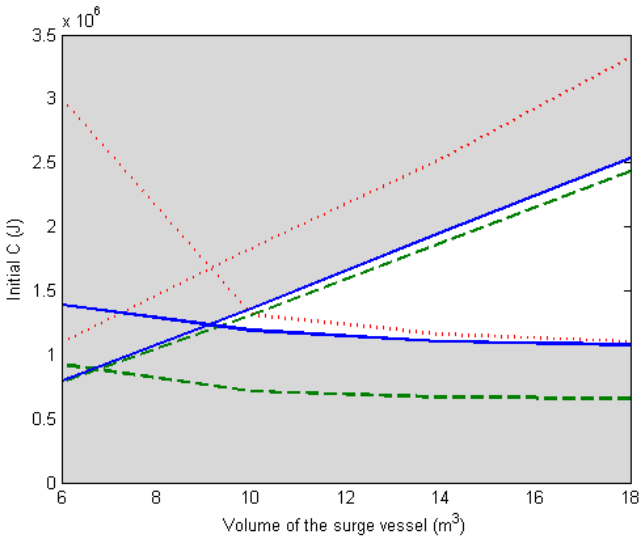

Figure 4.4: The optimization graph that shows the minimal volume of the surge vessel that has to be used for a system and its initial $pV = C$ value. The dotted line show the calculations with a Laplace coefficient of $n = 1.4$, the dashed line the calculations with a Laplace coefficient with $n = 1.0$ and the solid line the calculations with the RHT model. The grey area indicates the surge vessel volumes and their initial C values that give unacceptable water levels or pipe pressures.

adiabatic and isothermal lines. That means that the minimal volume calculated with the RHT model is around 10% smaller than the calculations with the polytropic model.

These calculations have also been done with the RHT model for isolated tank walls. These results were very similar to the result in Figure 4.4, with a slight difference in the upper bound of the acceptable triangle.

4.2 Validation of model Shuweihat

The data that have been obtained from the tests in the Arab Emirates have been compared to the different graphs that were obtained running the RHT model and the polytropic process model WANDA uses. The different graphs can be seen in Figure 4.5. The graph that is obtained from the tank with insulated walls is not included in this figure, because the walls of the tanks in Shuweihat are not insulated.

From the measurement data an initial $pV = C$ can be calculated, which lies around 38000 kJ. According to the design report of these surge vessels, the initial C value should be 28000 kJ $\pm$ 7 %. To make sure the model uses the same values as the experiment, a value of 38000 kJ is used to do these calculations.

In the different graphs in Figure 4.5 it can be seen that the pressure line from the measurement data decays along with the graph of the obtained adiabatic WANDA calculation and the RHT model, and then lies in between these lines and the isothermal line from WANDA. After 250 seconds the measured data shift between the RHT pressure line and

the adabatic pressure line. The measured volume values rises along with the RHT value and the adiabatic value and stays with the RHT line until 500 seconds. After that, the measurement data show an offset, which could be caused by the fact that the system has not been calibrated fully, so that the pressure wave propagation speed is not entirely accounted for. Furthermore, the measured system could have a leakage, so that the surge vessel drains more. This can be seen in the expanding volume after 500 seconds.

The temperature data from Shuweihat does not vary much, although a slight drop and rise in temperature can be seen at the same time as the temperature of the RHT model drops and rises. The small temperature variance could be caused by the location of the temperature sensor inside the surge vessel. If this sensor is placed near the tank wall, the thermometer can be heated by conduction or radiation and the data will be biased.

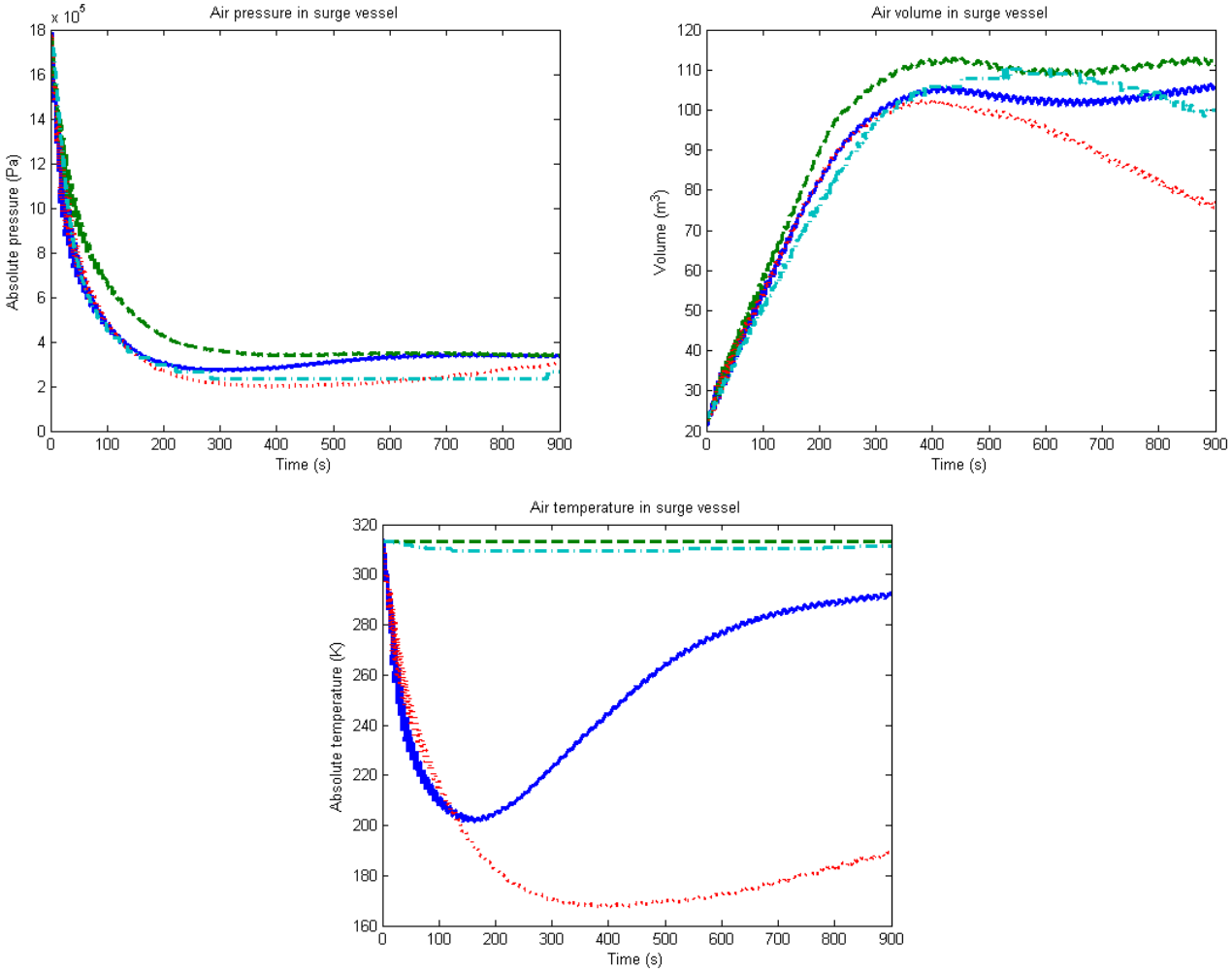

Figure 4.5: Values of air pressure, air volume and air temperature of the RHT equation with input from the Shuweihat surge vessels (solid line) compared to the measured data from Shuweihat (dash-dotted line) and the calculations from the WANDA model with $n = 1.0$ (dashed line) and $n = 1.4$ (dotted line).

4.3 Mathematical model

When Equation (3.14) is implemented in MATLAB, for the temperature in the height of the surge vessel Figure 4.6a is obtained. In this graph it can be seen that the bottom of the air pocket is warmed up much faster than the ceiling of the air pocket. This is because the convective influences are only present at the bottom; the ceiling of the tank only warms up due to conduction. The source term, which is implemented following (3.21), has an outcome that is shown in Figure 4.6b.

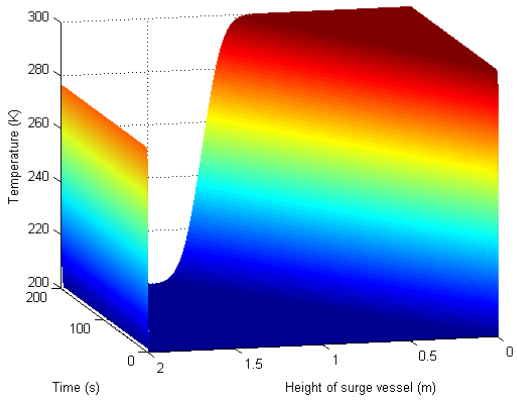

(a) Temperature distribution without source term.

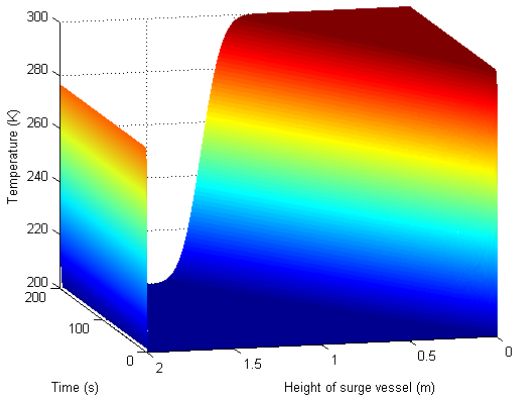

(b) Temperature distribution with source term.

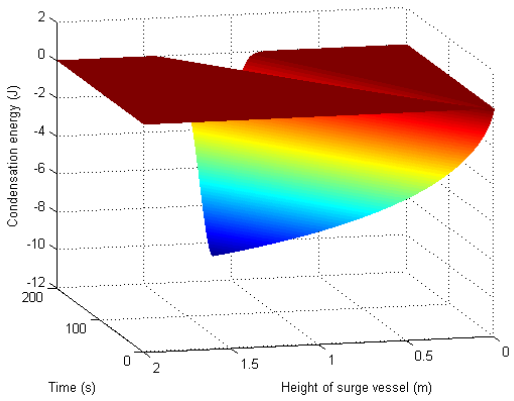

(c) The energy that is added to the surge vessel by the source term. This graph shows the net effect of the evaporation heat.

Figure 4.6: A surface representation of the temperature inside the tank in the z-direction. The model time is 200 seconds. The starting temperature is 200 K and both the water and the wall temperatures are 300 K.

The difference between Figures 4.6a and 4.6b is hard to see. This difference is made visible in Figure 4.6c, which shows the difference between the graph in Figure 4.6b and Figure 4.6a, multiplied with the mass and the specific heat of the air. This graph shows the energy effect the condensation term has on the rise in temperature. The graph is

completely negative which is the case because when the temperature rises, the water in the air pocket will evaporate and this phenomenon will cost energy. Therefore the rise in temperature will be lower in the graph with a source term.

The effect of evaporation is very low. In Figure 4.6c, the difference in temperature due to condensation heat can be seen in each point and on each time step. When this graph is multiplied with the volume, density and specific heat, the energy contribution is taken into account. A summation over all points and all time steps will give a better idea of the total evaporation energy. From the data it can be calculated that on average, per second 502 J is needed for the evaporation, with a total of $1.00 \cdot 10^4$ J.

4.3.1 Errors

The order of the error will be given by p from Equation (3.25). Because the centered difference used is of order 2, but the upwind difference method and the time difference are both order 1, a p value of around 1 is expected.

From the error analysis results were obtained that can be found in Table 4.2. From this table it can be seen that when the grid is rough and many time steps are used, the error is very high. The error of the x-domain dominates the error of the t-domain, because for a varying amount of time steps, the error stays large.

For a grid size that is about equal to the amount of time steps, the best results are obtained. In this case the order of the error is indeed approximately equal to 1, as was expected. The two results with grid size 2000 have errors that differ a factor two, which can be explained by the doubled amount of time steps; if the calculation has twice as much steps, the error will be two times as high.

Table 4.2: Error order calculations of the mathematical model. the error calculations have been done with different grid sizes and different amounts of time steps.

Grid size	Time steps	Order of error	Error
200	200 000	0.1067	662.8
200	2 000 000	0.1066	663.7
500	1 000 000	0.224	224
1000	1 000	0.7934	74.36
2000	1 000	1.07867	33
2000	2 000	0.9997	62.05

Chapter 5

Conclusions and Recommendations

In short, answering the question that was stated in the Introduction of this thesis, the Rational Heat Transfer (RHT) model can be used to model the behavior of surge vessels in piping systems. This approach gives a way to predict the behavior of the vessels without running the WANDA model twice to obtain only the minimum and maximum behavior. The statement of Graze (1968) that the polytropic model is sufficient, but not accurate enough to model the behavior of surge vessels, can be considered true, because added heat to the system does have a large effect. The minimal volume of a surge vessel needed to ensure the safety of the piping system becomes smaller if in the calculations the RHT model is used. In the following sections, these conclusions are explained in more detail.

5.1 RHT model

In conclusion, from the results of the Rational Heat Transfer (RHT) model it can be seen that this model gives logical and physically possible values for pressure, volume, and temperature. The RHT equation is indeed an alternative way to model the behavior of surge vessels. These outcomes suggest that the air volume in the surge vessel can be predicted more efficiently than with the polytropic process formula (2.3), because only one calculation is needed, instead of two calculations for isothermal and adiabatic behavior.

The Laplace coefficient that was always known to be somewhere between 1.0 and 1.4 for isothermal and adiabatic expansion can not be considered constant. According to the RHT model, the value will start on $n = 1.4$ but will gradually drop. At the start of the expansion, the temperature drop is still small, so the heat will not flow yet. This looks like a system without heat flow, so the process will have an adiabatic Laplace coefficient. As the heat flow becomes larger, the system can not be considered adiabatic, and the Laplace coefficient will drop.

From the heat flow results from Section 4.1.2 the conclusion can be drawn that the heat flows inside the surge vessel are indeed significant compared to the total work done by the

air expansion. As stated by Graze (1968), especially the convective heat flow is a large part of the energy balance inside the vessel, which should not be neglected.

At last, from Section 4.1.4 it can be concluded that the RHT model outperforms the simulations with isothermal or adiabatic behavior. The difference in performance is most obvious in the surge vessel air volume variable, which is 10 % smaller with the RHT model calculation than with the polytropic model calculation. In this example the absolute difference is not that big, but in larger systems, a 10 % smaller surge vessel volume may mean less surge vessels. This will in the end reduce the construction costs of the pipeline system.

5.1.1 Comparison to measurement data Shuweihat

As there are results available from an actual surge vessel, the data from this vessel placed in Shuweihat can be analyzed. The results that were introduced in Section 4.2 show that the volume expansion and the pressure drop can be modeled very accurately. They both show a small offset that can be caused by a slight difference in the eight surge vessels that were placed in Shuweihat. These surge vessels do not behave exactly the same, so there could be a difference between the displayed surge vessel and the measured surge vessel.

The temperature values of the measured data are nearly constant. The temperature sensor is located near the ceiling or the tank, due to heat conduction and radiation from the roof, the sensor could be influenced. Furthermore, radiation could play a more important role than expected because the temperatures are higher than in the example of the piping network in Zwolle.

In conclusion, this means that the RHT model could be useful to predict the behavior of the surge vessel. To validate this further, more measurements are needed, for instance with a temperature sensor on different locations inside the surge vessel.

5.2 Mathematical model

From the mathematical model it can be concluded that convective heat transfer has most important influence on the air temperature in a surge vessel, when the air is expanded. Heat conduction and evaporation also have their influence, but these influences are less than the influence of convection. This conclusion fits into the estimations made in Chapter 3. The amount of heat needed for evaporation of the air also fits with the data from the RHT model. Although the condensation from the RHT model adds heat to the system, it is important that the values of the two heat contributions are of the same order, because the processes are the same but reversed.

Another conclusion that can be drawn, is that the time needed to warm up the volume of air, is much longer than 200 seconds. This means that the location of the temperature sensor makes a difference. A two-dimensional model should be made and experiments should be done to check what position in the surge vessel gives the most accurate temperature values.

In this model radiation has not been taken into account, because the radiation is not the most important heat contribution for temperatures under 300 K. For models of surge

vessels in climates with higher temperatures than 300 K, radiation should be accounted for.

5.3 Recommendations

As stated in Section 5.1 the most important follow up is doing more tests with surge vessels, to validate the results of the RHT model. In this thesis, one experiment has provided measurement data, but more validation is important to get an idea of the accuracy of the RHT model.

Secondly, when placing vessels in regions with warmer climates and higher air temperatures, it could be important to account for radiation heat transfer, too. In the estimation made in this thesis, the radiation term was small in comparison to the other heat transfer terms, but a higher accuracy could be reached if radiation is implemented into the model.

For the mathematical model of the surge vessel, some extensions could be made to make the model more applicable to the behavior of surge vessels. These include a two-dimensional approach, variable pressure and volume values, and a radiation term. Furthermore, the convective term is not taken into account properly, because convection can not be considered as a process that can be measured from grid point to grid point, but has to be taken into account globally in the whole tank. That means that the mathematical approach shows some physical errors, while the mathematics behind it is correct.

At last, other upwind difference methods could be used to get an error order of 2 instead of 1, another time-integration method could also help to achieve this. The source term could be linearized in a different way to obtain a smaller error.

References

Ellis, J. (2008). *Pressure transients in water engineering; a guide to analysis and interpretation of behaviour*. Thomas Telford Publishing Limited.

Ferziger, J. H., & Peric, M. (2002). *Computational methods for fluid dynamics* (3rd ed.). Springer-Verlag Berlin Heidelberg.

Fitzgerald, R., & Van Blaricum, V. L. (1998, september). Water Hammer and Mass Oscillation (WHAMO) 3.0 user's manual [Computer software manual].

Graze, H. R. (1967). *A rational approach to the thermodynamic behaviour of air chambers* (Unpublished doctoral dissertation). University of Melbourne.

Graze, H. R. (1968). Rational thermodynamic equation for air chamber design. *Conference on Hydraulics and Fluid Mechanics*.

Graze, H. R. (1971). New air chamber characteristics. *Fourth Australian Conference on Hydraulics and Fluid Mechanics*.

Haberman, R. (2014). *Applied partial differential equations with fourier series and boundary conditions* (5th ed.). Pearson Education Limited.

Kuzmin, D., & Möller, M. (2004). *Algebraic flux correction I; Scalar conservation laws*. Institute of applied Mathematics, University of Dortmund.

Leruth, P., Pothof, I., & Naja, F. (2012). Validation of the surge model and lessons learnt from commissioning of the Shuweihat Water Transmission Scheme, UAE. *TRANSCO Publications*.

Lowe, P. R. (1976). An approximating polynomial for the computation of saturation vapor pressure. *Journal of applied meteorology*, *10*.

Moran, M. J., & Shapiro, H. N. (2010). *Fundamentals of engineering thermodynamics* (Sixth Edition ed.). John Wiley & Sons, Inc.

Patankar, S. (1980). *Numerical heat transfer and fluid flow.* Hemisphere Publishing Corporation.

Thorley, A. R. D. (2004). *Fluid transients in pipeline systems; a guide to the control and suppression of fluid transients in liquids in closed conduits* (Second ed.). Professional Engineering Publishing Limited.

Vaisala. (2013). *Humidity conversion formulas; calculation formulas for humidity.* Vaisala Oyj P.O. Box 26 FI-00421 Helsinki Finland.

Van den Akker, H., & Mudde, R. (2008). *Fysische transportverschijnselen.* VSSD.

Van der Zwan, S., Rudolph, D., Balkema, S., Pothof, I., & Leruth, P. (2012, October). Optimization of surge protection for a large water transmission scheme in abu dhabi. *11th International conference on Pressure Surges, Lisbon*.

Vuik, C., van Beek, P., Vermolen, F., & van Kan, J. (2006). *Numerieke methoden voor differentiaalvergelijkingen.* VSSD.

Wanda 4.2 user manual [Computer software manual]. (2013, June).

Appendix A

Used constants

Table A.1: List of used constants and values in calculations.

Symbol	Description	Value	Unit
a_{air}	Thermal diffusion coefficient	$2.119 \cdot 10^{-5}$	m^2 / s
a_{steel}	Thermal diffusion coefficient	$4 \cdot 10^{-6}$	m^2 / s
$C_{p,air}$	Specific heat with constant pressure	1002	J / (kg K)
$C_{p,steel}$	Specific heat with constant pressure	490	J / (kg K)
g	Gravitational acceleration	9.81	m / s^2
$h_{ev,water}$	Evaporation enthalpy	2200	kJ / kg
R	Ideal gas constant	8.314	Pa m^3 / (mol K)
ϵ_{steel}	Emission coefficient for radiation	0.7	-
γ	Ratio of specific heats; $\frac{C_p}{C_v}$	1.4	-
λ_{air}	Heat conductivity coefficient	0.0257	J/(s m K)
λ_{steel}	Heat conductivity coefficient	16	J/(s m K)
ν	Kinematic viscosity	$1.343 \cdot 10^{-5}$	m^2/s
σ	Stefan-Boltzmann coefficient	$5.67 \cdot 10^{-8}$	J / (s m^2 K^4)
Pr_{air}	Prandtl number	0.72	-

Appendix B

Matlab codes

B.1 Work done by expanding air pocket

```
%total work done by expanding air pocket
C = 3.676*4.081*10^5;
p1 = @(V) C./V.^1.0;
W1 = integral(p1,3.676,12.12);
C14 = 3.676^1.4*4.081*10^5;
p14 = @(V) C./V.^1.4;
W14 = integral(p14,3.676,9.217);
```

B.2 Tank wall heating

```
%Heat transfer to steel on steel-air interface
D=2;
Tw=288;
Ta=199;
a = 4*10^-6;
Tis = @(t) (16*D*Tw + 20*0.0257*sqrt(pi*a*t)*Ta)./(20*0.0257*sqrt(pi*a*t)+16*D);
plot(Tis(1:1:200))
xlabel('Time (s)');
ylabel('Temperature (K)');
axis([0 200 286 289]);
```

B.3 Heat transfer processes

```
%Estimation of different heat transfer processes, code is written in Dutch
%Keteleigenschappen n=1.4
tijd = 100; %s
grondoppervlak = 3; %m2
```

```
ketelhoogte = 6; %m
Vbegin = 3.676;
waterhoogte = ketelhoogte - Vbegin/grondoppervlak; %m
straal = sqrt(grondoppervlak / pi); %m
diameter = 0.5 * straal; %m
wandoppervlak = 2*pi*straal*(ketelhoogte-waterhoogte);
wanddikte = 0.045;%m
pbegin = 4.081; %wanda waarde
peind = 1.127; %wanda waarde

Veind =  9.217; %wanda waarde
wandtemperatuur = 288; %K
luchttemperatuur = wandtemperatuur * Veind*peind/Vbegin/pbegin; %K, gaswet
deltaT = (wandtemperatuur-luchttemperatuur);

%Stofeigenschappen lucht
pwbegin = 0.01705;
pweind = 1.29*10^-4;
labda = 0.0262;%warmtegeleiding lucht
cplucht = 1002;
a=2.11*10^(-5);%warmtevereffening
nu = 1.343*10^-5; %Kinematische viscositeit bij 275 K

%Stofeigenschappen staal
cpstaal = 490;
dichtheids = 7800;

%Stofeigenschappen water
enthalpie = 2200000; %verdamping van water
dichtheidw = 1000;
cpwater = 4180;
g=9.81;
R = 8.314;


%Geleiding penetratietheorie
fluxgeleiding = labda*deltaT/(sqrt(pi*a));
fluxgeleidingf = @(t) labda*deltaT./(sqrt(pi*a.*t)); %gedeeld door wortel t
Egeleiding = integral(fluxgeleidingf,0,tijd) * (wandoppervlak+2*grondoppervlak)


%vrije convectie
Gr = diameter^3*g*deltaT/(nu^2 * luchttemperatuur) ;
Pr = 0.72;
Nuconvectie = 0.12 *(Gr*Pr)^(1/3); %Verticale vlakke plaat convectie
fluxconvectie = Nuconvectie * labda * deltaT / diameter; %Newtons afkoelingswet
Econvectie = fluxconvectie * (2*grondoppervlak + wandoppervlak) * tijd

% Condensatie
dichtheidl1 = (pbegin * 0.0289*10^5 + pwbegin*0.018*10^5) / R  / wandtemperatuur;
massafractiebegin = 0.622*pwbegin/(pbegin-pwbegin);
massafractieeind = 0.622*pweind/(peind-pweind);
massalucht = Vbegin * dichtheidl1;
massawater = (massafractiebegin - massafractieeind) * massalucht;
Econdensatie = enthalpie * massawater
dichtheidl2 = (peind * 0.0289*10^5 + pweind*0.018*10^5) / R  / luchttemperatuur;
luchttemperatuur2 = (cplucht *Veind *dichtheidl2 * luchttemperatuur + cpwater...
    *massawater*luchttemperatuur +massawater*enthalpie)/ (cpwater *massawater...
```

```
    + cplucht*massalucht);

%Warmtevereffening Stalen wand en water
massastaal = (wandoppervlak+grondoppervlak*2)*wanddikte *dichtheids;
luchttemperatuur3 = (cplucht *Veind *dichtheidl2 * luchttemperatuur + cpstaal...
    *massastaal*wandtemperatuur)/ (cpstaal *massastaal + cplucht*massalucht);
```

B.4 Rational Heat Transfer Equation

```
function [pend,Tend,Qconduction,Qconvection,Qcondensation] = ...
    rht(volumechange,V,p,T,pilast,Tilast,time,timestep,SV)

tempEx = 323;%K
enthalpy = 2200000;
labda = 0.0262;
R = 8.314;
gamma = 1.4; %ratio of specific heats
a = 2.119 *10^-5; %heat diffusion coefficient
Pr = 0.72; %Prandtl
g = 9.81;
kinematicViscosity = 1.343*10^-5;

%Formula partial vapor pressure
a_0 =  6984.505294;
a_1 = -188.9039310;
a_2 =  2.133357675;
a_3 = -1.288580973 * 10^-2;
a_4 =  4.393587233 * 10^-5;
a_5 = -8.023923082 * 10^-8;
a_6 =  6.136820929 * 10^-11;
pw= @(T) (a_0 + a_1*T +a_2*T.^2 +a_3*T.^3 +a_4*T.^4 + a_5*T.^5 +a_6*T.^6)*100;


%Properties Surge Vessel
A = SV.area; %m^2, floor surface
diameter = sqrt(4*A/pi);
radius = 0.5 * diameter;
Z = V / A;


massfraction(1) = 0.622*pw(Tilast)/(pilast-pw(Tilast));
densityair = (p * 0.0289 + pw(T)*0.018) / R  / T;
massfraction(2) = 0.622*pw(T)/(p-pw(T));
massair = V * densityair;
masswater = -(massfraction(2) - massfraction(1)) .* massair;
Qcondensation = masswater * enthalpy;
Qconduction = labda*(tempEx - T).*(A +A + 2*pi*radius*Z)/sqrt(pi*a*time);
Gr = diameter^3*g*(tempEx-T)./(kinematicViscosity^2 * T);
Nu = 0.12* (Gr*Pr).^(1/3); %vertical plate convection
Qconvection = Nu .* labda .* (tempEx-T) ./ diameter .*(A + 2*pi*radius.*Z);
dQdt = - Qcondensation- Qconduction-Qconvection;
pressurechange = (-gamma *p/V *volumechange/timestep - (gamma-1)/V*dQdt)*timestep;
pend = p + pressurechange;
Vend = V + volumechange;
Tend = Vend*pend*T/V/p; %ideal gas law
```

B.4.1 Minimum Surge vessel volumes

```
%Function to make graphs of optimized surge vessel volumes of RHT model
%compared with volumes of polytropic model.
tic;
initialC = 1500e3; %An acceptable initial value is needed
area = [1 10/6 14/6 18/6];
%Acceptable C values
Cupperbound = [9.002 *4.49*10^5,9.002 *4.49*10^5, 12.6*4.49*10^5, 16.2*4.49*10^5];
Clowerbound = [0.1 *3.97*10^5,0.1667*3.97*10^5, 0.2333*3.97*10^5,0.3*3.97*10^5];

%Calculation for minimum pressure value and minimum water level
for i = 1:4
    Cp(2) = Clowerbound(i);
    Cp(3) = Cupperbound(i);

    [p(2), xf(2)] = WandaenginerunnenSVoptim(1,1.0,Cp(2),area(i));
    [p(3), xf(3)] = WandaenginerunnenSVoptim(1,1.0,Cp(3),area(i));
    pstart = p;
    xfstart = xf;

    %check if p and Wl OK
    if p(2) < 0 && p(3)<0
       Cp(1) = 0;
    elseif p(2) > 0 && p(3)>0
        Cp(1) = Clowerbound(i);
    else
        Cp(1) = (Cp(2) + Cp(3))/2;

        eps = 1;
        while eps > 0.01
            [p(1), xf(1)] = WandaenginerunnenSVoptim(1,1.0,Cp(1),area(i));
            if p(1)>0
                Cp(3) = Cp(1);%upper goes down
                Cp(1)= (Cp(3)+Cp(2))/2;
                eps = abs(Cp(1)-Cp(3)) /Cp(3);
            else
                Cp(2) = Cp(1);%lower goes up
                Cp(1)= (Cp(3)+Cp(2))/2;
                eps = abs(Cp(1)-Cp(2)) /Cp(2);
            end

        end
    end

    Cxf(2) = Clowerbound(i);
    Cxf(3) = Cupperbound(i);

    p = pstart;
    xf=xfstart;

    %check if p and Wl OK
    if xf(2) < 0.6 && xf(3)<0.6
       Cxf(1) = 0;
    elseif xf(2) > 0.6 && xf(3)>0.6
        Cxf(1) = Cupperbound(i);
```

```
    else
        Cxf(1) = (Cxf(2) + Cxf(3))/2;

        eps = 1;
        while eps > 0.01
            [p(1), xf(1)] = WandaenginerunnenSVoptim(1,1.0,Cxf(1),area(i));
            if xf(1)>0.6
                Cxf(2) = Cxf(1);%lower goes up
                Cxf(1) = (Cxf(3)+Cxf(2))/2;
                eps = abs(Cxf(1)-Cxf(2)) /Cxf(2);
            else
                Cxf(3) = Cxf(1);%upper goes down
                Cxf(1) = (Cxf(3)+Cxf(2))/2;
                eps = abs(Cxf(1)-Cxf(3)) /Cxf(3);
            end
        end
    end


    Cprer_P(i) = Cp(1);
    Cprer_X(i) = Cxf(1);
end

toc
```

B.5 RHT Wanda connection

```
function [druk, volume, temperatuur,Qconduction,Qconvection, Qcondensation]...
    = Wandaenginerunnen


wandacase2 = 'D:\test\network.wdi';
wandaenginedir2 = 'D:\test\wandaengine\';
%to start the wandaengine you need to be in the wandaengine dir.
cd(wandaenginedir2)

%load Wanda engine into the memory
asminfo2 =  NET.addAssembly([wandaenginedir2 'Deltares.Wanda.WandaEngine.dll']);
wandarun2 = Deltares.Wanda.WandaEngine();

% initialiseren van het model
wandarun2.Initialize(wandacase2);
% steady draaien
wandarun2.PerformTimeStep();
% tijd stap ophalen
dt = wandarun2.GetValue('GENERAL',' ','Time step');
ST = 200;
timesteps = ST/dt;
%%Surge vessel sizes:
Top_level     = 6.00000;
Bottom_level  = 0.000000;
Chamber_area  = 3.000;
Initial_C     = 1500e3;
Laplace       = 1.400;
RHO_F         =  1000;
GRAV          = 9.81;
PATMOS        = 1.014e5;
SV.height = Top_level -Bottom_level;
SV.area = Chamber_area;
H_INI = wandarun2.GetValue('BOUNDH','B2','Head 1');
A  = RHO_F*GRAV*Chamber_area;
B  = PATMOS*Chamber_area;
BB = -A*Top_level-A*H_INI-B;
CC = A*H_INI*Top_level+B*Top_level-Initial_C;
XF(1) = (-BB - sqrt (BB*BB-4*A*CC))/(2*A);
P(1) = ( H_INI - XF ) * RHO_F * GRAV + PATMOS;
P(2) = ( H_INI - XF ) * RHO_F * GRAV + PATMOS;
V_AIR(1) = ( Initial_C/P(1) );
V_LIQ(1) = Chamber_area * ( Top_level - Bottom_level ) - V_AIR(1);
C = P(1) * ( V_AIR(1) ^ Laplace );
H(1) = H_INI;
QAIRV(1) = 0;
TEMP(1) = 288;
TEMP(2) = 288;
Qconvection = 0;
Qcondensation= 0;
Qconduction = 0;
for i = 1:timesteps
    %getting the discharge of the SV
    QAIRV(i+1) = wandarun2.GetValue('BOUNDH','B2','Discharge 1')/3600;
    V_AIR(i+1) = V_AIR(i) +  QAIRV(i+1) * dt;
```

```
    V_LIQ(i+1) = V_LIQ(i) -  QAIRV(i+1) * dt;
    XF(i+1)    = XF(i)    -  QAIRV(i+1)/Chamber_area * dt;
    %P(i+2) = C/V_AIR(i+1) ^ Laplace;
    %TEMP(i+1) = TEMP(i)*P(i+2)*V_AIR(i+1) /(P(i+1) * V_AIR(i));
    [P(i+2),TEMP(i+2),Qconduction(i),Qconvection(i),Qcondensation(i)] ...
        = rht(QAIRV(i+1)*dt,V_AIR(i),P(i+1),TEMP(i+1),P(i),TEMP(i),dt*i,dt,SV);
    H(i+1)  =  ( P(i+2) - PATMOS)/( RHO_F * GRAV ) +  XF(i+1);
    wandarun2.SetValue('CON','C1','Value',H(i+1));
    %running timestep and catching the error so wanda can be stopped
    %safely.
    try
        wandarun2.PerformTimeStep();
    catch e
        display('Wanda calculation stopped due to error')
        break
    end
end
druk = P;
temperatuur = TEMP;
volume = V_AIR;
%finish the simulation when an error has occured.

wandarun2.Finish();



%This code is used to make the graphs for the obtained WANDA values
tijd = 0.05:0.05:200;
S = load('plaatjesfiles191114');
R = load('plaatjesfiles181114');
linewidth = 2.5;
figure(1);
plot(tijd,S.druk(2:4001),'-','LineWidth',linewidth)
hold all
plot(tijd,R.druk10(2:4001),'--','LineWidth',linewidth)
plot(tijd,R.druk14(2:4001),':','LineWidth',linewidth)
plot(tijd,S.drukisowater(2:4001),'-.','LineWidth',linewidth)
%legend('RHT','n=1.0','n=1.4')
title('Air pressure in surge vessel')
xlabel('Time (s)')
ylabel('Absolute pressure (Pa)')

figure(2);
plot(tijd,S.temperatuur(2:4001),'-','LineWidth',linewidth)
hold all
plot(tijd,R.temperatuur10(1:4000),'--','LineWidth',linewidth)
plot(tijd,R.temperatuur14(1:4000),':','LineWidth',linewidth)
plot(tijd,S.temperatuurisowater(2:4001),'-.','LineWidth',linewidth)
title('Air temperature in surge vessel')
xlabel('Time (s)')
ylabel('Absolute temperature (K)')

figure(3);
plot(tijd,S.volume(1:4000),'-','LineWidth',linewidth)
hold all
plot(tijd,R.volume10(1:4000),'--','LineWidth',linewidth)
plot(tijd,R.volume14(1:4000),':','LineWidth',linewidth)
plot(tijd,S.volumeisowater(1:4000),'-.','LineWidth',linewidth)
```

```
title('Air volume in surge vessel')
xlabel('Time (s)')
ylabel('Volume (m^3)')

figure(4);
plot(tijd,log((S.volume(1)^1.4*S.druk(1))./S.druk(2:4001))./log(S.volume),...
    '-','LineWidth',linewidth)
hold all
plot(tijd,log((R.volume10(1)^1*R.druk10(1))./R.druk10(2:4001))./log(R.volume10),...
    '--','LineWidth',linewidth)
plot(tijd,log((R.volume14(1)^1.4*R.druk14(1))./R.druk14(2:4001))./log(R.volume14),...
    ':','LineWidth',linewidth)
plot(tijd,log((S.volumeisowater(1)^1.4*S.drukisowater(1))./S.drukisowater(2:4001))...
    ./log(S.volumeisowater),'-.','LineWidth',linewidth)
plot(tijd,log((S.volume(1)^1*S.druk(1))./S.druk(2:4001))./log(S.volume),...
    '-','LineWidth',linewidth)
title('Laplace coefficient')
xlabel('Time (s)')
ylabel('Laplace coefficient (-)')

figure(5);
plot(0.1:0.05:200,S.Qconduction,'-','LineWidth',linewidth);
hold all
plot(0.1:0.05:200,S.Qconvection,'--','LineWidth',linewidth);
plot(0.1:0.05:200,S.Qcondensation,':','LineWidth',linewidth);
plot(0.1:0.05:200,S.druk(3:4001).*(S.volume(2:4000) - S.volume(1:3999)),...
    '-.','LineWidth',linewidth);
xlabel('Time (s)')
ylabel('Energy (J)')
```

B.6 Mathematical model

```
%Temperature calculation in a 1D surge vessel
tic;
%Definition of used constants
Twall = 300;
Twater = 300;
T0 = 200;
height = 2;
gridZ = 200;
time = 200;
timestep = 0.01;
steps = time/timestep;
R = 1;
h = height/gridZ;
T = zeros(gridZ,steps);
A = 2*pi*R;
V = 2*pi*R*h;
rho = 1.293;
cp = 1002;
enthalpy = 2200000;
p = 2*10^5;
labda = 0.0257;
Nu = 300;
Diam = 1;
```

```
g=9.81;
T(:,1) = T0;
kinematischeViscositeit = 1.343*10^-5;
Pr = 0.72;
%Formule partial vapor pressure

pw= @(T) (6984.505294 + -188.9039310*T +2.133357675*T.^2 +-1.288580973 *...
    10^-2*T.^3 +4.393587233 * 10^-5*T.^4 + -8.023923082 * 10^-8*T.^5 +...
    6.136820929 * 10^-11*T.^6)*100;


%Formule Nusselt
%Nu = @(T) 0.17* (D^3*g*(Twater-T(:,i))./(kinematischeViscositeit^2 * T)*Pr)...
    %.^(1/3)/T; %Horizontale vlakke plaat convectie

%Simplified problem, only the matrices are defined
Diff = (diag(ones(gridZ-1,1),-1)+diag(-2*ones(gridZ,1),0)+...
    diag(ones(gridZ-1,1),1))/h^2;
Conv = (diag(1*ones(gridZ-1,1),1)+diag(-1*ones(gridZ,1),0))/(h);
rest = zeros(gridZ,1);
%rest(1) = - 1/(2*h);
rest(1) = rest(1) + 1/h^2 ;%;
rest(end) = 1/(h);
rest(end) = rest(end) + 1/h^2 ;%;
J= diag(ones(gridZ,1))/timestep;

D = A*labda*Diff;
C = Nu*labda*A/Diam*Conv;
r = zeros(gridZ,1);

%Convection only takes place on the water level, which is implemented on Z=2
r(1) = r(1) + Twall*(A*labda/h^2);
r(end) = r(end) + Twater*(A*labda/h^2+Nu*labda*A/Diam/(h));
I = J*rho*cp*V/h;
P = @(T) diag(0.622*V*enthalpy*rho*timestep/h * pw(T)./(T.*(p-pw(T))));
Tq=T;
Td=T;
for i=1:steps
    %Solving for Diffusion and Convection
    Tq(:,i+1) = (I-D)\((I+C)*Tq(:,i)+r);
    %Fixed point iteration
    Ttemp = T(:,i);
    residual = (I+C+P(T(:,i)))*T(:,i)+r -(I-D+P(Ttemp))*Ttemp;
    res0 = norm(residual);
    for ite=1:1000
       deltaT = (I-D+P(Ttemp))\residual;
       Ttemp = Ttemp+deltaT;
       residual = (I+C+P(T(:,i)))*T(:,i)+r -(I-D+P(Ttemp))*Ttemp;
       res = norm(residual);
       mean(Ttemp);
       if res*1000 < res0
           T(:,i+1) = Ttemp;
           break
       end
    end
end
%Figure composition
az=-104;
```

```
el=14;
%Turning around the values, as the water level was considered at the
%ceiling and the other way around
T = flip(T);
figure(1);
surf(0:timestep:time,h:h:2,T)
shading interp
view([az,el])
ylabel('Height of surge vessel (m)')
xlabel('Time (s)')
zlabel('Temperature (K)')
Tq = flip(Tq);
figure(2);
surf(0:timestep:time,h:h:2,Tq)
shading interp
view([az,el])
ylabel('Height of surge vessel (m)')
xlabel('Time (s)')
zlabel('Temperature (K)')
figure(3);
surf(0:timestep:time,h:h:2,(T-Tq)*rho*V*cp)
shading interp
view([az,el])
ylabel('Height of surge vessel (m)')
xlabel('Time (s)')
zlabel('Condensation energy (J)')
diff = (T-Tq)*rho*V*cp;
sumQ = sum(diff);
meanQ = mean(sumQ);
totalQ = sum(sumQ);
```

B.6.1 Error analysis

```
%Error analysis of heat equation
%When the grids are 'fine enough', the following method will work.
%I assume that the grid will be halved; r=2;

gridh = 999;
grid2h = 499;
grid4h = 249;
timestep = 1e-2;

T4h = temperaturedistribution(grid4h,4*timestep);
T2h = temperaturedistribution(grid2h,2*timestep);
Th = temperaturedistribution(gridh,timestep);

t2h = (T2h(1:end-1,end)+T2h(2:end,end))/2;
T2ha = reshape([T2h(1:end,end)'; t2h' 0], 2*size(T2h,1), 1);
T2ha(end) = [];

t4h = (T4h(1:end-1,end)+T4h(2:end,end))/2;
T4ha = reshape([T4h(1:end,end)'; t4h' 0], 2*size(T4h,1), 1);
T4ha(end) = [];

p = log(norm(T2h(1:end,end)-T4ha)/norm(Th(1:end,end)-T2ha))/log(2);
errorh = norm(Th(1:end,end)-T2ha)/(2^p - 1);
```

```
%Tussenpunten berekenen in plaats van 1:2:end



%Temperature on the right and numerical math way
function [Th] = temperaturedistribution(gridh, timestep)
tic;
Twall = 300;
Twater = 300;
T0 = 200;
height = 2; %Z=0 is de bovenkant van de ketel, Z=10 de onderkant
gridZ = gridh;
time = 100;

steps = round(time/timestep);
R = 1;
h = height/gridZ;
T = zeros(gridZ,steps);
A = 2*pi*R;
V = 2*pi*R*h;
rho = 1;
cp = 1002;
enthalpy = 2200000;
p = 2*10^5;
labda = 0.0257;
Nu = 300;
D = 1;
g=9.81;
T(:,1) = T0;
kinematischeViscositeit = 1.343*10^-5;
Pr = 0.72;
%Formule partial vapor pressure
% a_0 =  6984.505294;
% a_1 = -188.9039310;
% a_2 =  2.133357675;
% a_3 = -1.288580973 * 10^-2;
% a_4 =  4.393587233 * 10^-5;
% a_5 = -8.023923082 * 10^-8;
% a_6 =  6.136820929 * 10^-11;
pw= @(T) (6984.505294 + -188.9039310*T +2.133357675*T.^2 +-1.288580973 *...
    10^-2*T.^3 +4.393587233 * 10^-5*T.^4 + -8.023923082 * 10^-8*T.^5 +...
    6.136820929 * 10^-11*T.^6)*100;


%Versimpeld probleem
Diff = (diag(ones(gridZ-1,1),-1)+diag(-2*ones(gridZ,1),0)+...
    diag(ones(gridZ-1,1),1))/h^2;
Conv = (diag(1*ones(gridZ-1,1),1)+diag(-1*ones(gridZ,1),0))/(h);
rest = zeros(gridZ,1);
%rest(1) = - 1/(2*h);
rest(1) = rest(1) + 1/h^2 ;%;
rest(end) = 1/(h);
rest(end) = rest(end) + 1/h^2 ;%;
J= diag(ones(gridZ,1))/timestep;

K = A*labda*Diff;
L = Nu*labda*A/D*Conv;
r = zeros(gridZ,1);
```

```
%r = condensationheat(Tn,Tn_1,V,p)';
%Convectie vindt alleen plaats aan het water, dat bevindt zich op Z=10
r(1) = r(1) + Twall*(A*labda/h^2);%hier moet Q straks in (productieterm)
r(end) = r(end) + Twater*(A*labda/h^2+Nu*labda*A/D/(h));
I = J*rho*cp*V/h;
P = @(T) diag(0.622*V*enthalpy*rho*timestep/h * pw(T)./(T.*(p-pw(T))));
Tq=T;

for i=1:steps
    if mod(i,100) ==0
        i
    end
    %r = r + condensationheat(T(:,i),T(:,i-1),V,p);
    Tq(:,i+1) = (I-K)\((I+L)*Tq(:,i)+r);
    %T(:,i+1) = (J-Diff)\((J+Conv)*T(:,i)+rest);
    %error = 100;
    Ttemp = T(:,i);
    residual = (I+L+P(T(:,i)))*T(:,i)+r -(I-K+P(Ttemp))*Ttemp;
    res0 = norm(residual);
    for ite=1:1000
       deltaT = (I-K+P(Ttemp))\residual;
       Ttemp = Ttemp+deltaT;
       residual = (I+L+P(T(:,i)))*T(:,i)+r -(I-K+P(Ttemp))*Ttemp;
       res = norm(residual);
       mean(Ttemp);
       if res*1000 < res0
           T(:,i+1) = Ttemp;
           break
       end
    end
end
Th = [Twall*ones(1,steps+1); T; Twall*ones(1,steps+1)] ;

toc
```